A proteomic analysis unravels novel CORVET and HOPS proteins involved in *Toxoplasma gondii* secretory organelles biogenesis

Juliette Morlon-Guyot[1&], Hiba El Hajj[2&], Kevin Martin[1&], Adrien Fois[1&], Amandine Carrillo[1&], Laurence Berry[1&], Richard Burchmore[3], Markus Meissner[4,5], Maryse Lebrun[1], and Wassim Daher[1*]

[1]Dynamique des Interactions Membranaires Normales et Pathologiques, UMR5235 CNRS, INSERM, Université de Montpellier, Montpellier, France.

[2]Departments of Internal Medicine and Experimental Pathology, Immunology and Microbiology, American University of Beirut, Beirut, 1107 2020, Lebanon.

[3]Polyomics Facility, University of Glasgow, Glasgow, G12 8QQ, UK.

[4]Wellcome Centre for Molecular Parasitology, University of Glasgow, Glasgow, UK.

[5]Department of Veterinary Sciences, Experimental Parasitology, Ludwig-Maximilians-Universität, München, 80802, Munich, Germany.

*Corresponding author: E-mail: wassim.daher@univ-montp2.fr. Phone: + 33 04 67 14 49 27.

[&]These authors contributed equally to this work.

Functional characterization of CORVET and BDCP in *Toxoplasma*

Keywords: Apicomplexa, *Toxoplasma gondii*, Tet-inducible system, secretory organelles, invasion, CORVET, HOPS, anterograde trafficking, Vps8, Beach-domain containing protein, membranous fusion and fission events.

Abbreviations: Vps: Vacuole protein sorting; TATi-1: Trans-activator Trap identified; CORVET: class C core vacuole/endosome transport; HOPS: homotypic vacuole fusion and protein sorting; GAMA: Glycosylphosphatidylinositol-anchored micronemal antigen; PLP1: Perforin-like protein 1; SUB1: Subtilisin protease 1; RILP: Rab-interacting lysosomal protein; TGFBRAP1: Transforming growth factor beta receptor associated protein 1; BDCP: Beach-domain containing protein; ASP3: Aspartyl protease 3; CK3L: Yeast palmitoylated vacuolar membrane-localized casein kinase I Like; NAGT1: N-acetylglucosamine transferase; CPL: Cathepsin L protease; ARO: Armadillo repeats only protein; SAG1: Surface antigen 1; DHFR: Dihydrofolate reductase; CAT: Chloramphenicol acetyltransferase; GAP45: Glideosome-associated protein 45; PRF: Profilin.

Abstract

Apicomplexans use the endolysosomal system for the biogenesis of their secretory organelles, namely micronemes, rhoptries and dense granules. In *Toxoplasma gondii,* our previous *in silico* search identified the HOPS tethering but not the CORVET complex and demonstrated a role of Vps11 (a common component for both complexes) in its secretory organelles biogenesis. Herein, we performed Vps11-GFP-Trap pull-down assays and identified by proteomic analysis, not only the CORVET specific subunit Vps8, but also a BEACH domain-containing protein (BDCP) conserved in eukaryotes. We show that knocking-down Vps8 affects targeting of dense granule proteins, transport of rhoptry proteins, as well as the localization of the cathepsin-L protease vacuolar compartment marker. Only a subset of micronemal proteins are affected by the absence of Vps8, shedding light on at least two trafficking pathways involved in micronemes maturation. Knocking-down BDCP revealed a restricted and particular role of this protein in rhoptry and vacuolar compartment biogenesis. Moreover, depletion of BDCP or Vps8 abolishes parasite virulence *in vivo*. This study identified BDCP as a novel CORVET/HOPS-associated protein, playing specific roles and acting in concert during secretory organelle biogenesis, an essential process for host cell infection. Our results open the hypothesis for a role of BDCP in the vesicular trafficking towards lysosome-related organelles in mammals and yeast.

Introduction

Apicomplexans such as *Toxoplasma gondii* and *Plasmodium falciparum*, are obligate intracellular parasites that replicate inside a specific compartment named parasitophorous vacuole (PV), following the invasion of the host cell (Blader *et al*., 2014). Invasion is an orchestrated process that involves the sequential discharge of three unique secretory organelles called rhoptries, micronemes and dense granules, and plays a pivotal role for parasite maintenance and survival (Hakimi *et al*., 2017, Kemp *et al*., 2013, Mercier *et al*., 2015). During this process, microneme proteins (MICs) and Rhoptry Neck proteins (RONs) are first secreted and initiate the formation of a moving junction (MJ) required for host cell penetration (Frenal *et al*., 2017, Lamarque *et al*., 2014, Parker *et al*., 2016). Rhoptry bulb proteins (ROPs) are then secreted into the host cell. Some contribute to the formation of the parasitophorous vacuole (PV) in which the parasite intensively replicates, while others tightly control the host innate immune responses to assist parasite survival (Hakimi *et al*., 2017, Kemp *et al*., 2013). Dense granule proteins (GRAs) are involved in nutrient import, regulation of parasite antigen exposure at the PV, host gene expression modulation and immune responses prompted upon infection (Bougdour *et al*., 2014, Hakimi *et al*., 2015, Mercier *et al*., 2015).

Secretory organelles are *de novo* formed during each parasite replication cycle by budding and fusion of vesicles emerging from the Golgi (Breinich *et al*., 2009). These vesicles, proceed through the Trans-Golgi Network (TGN), Endosome-Like Compartments (ELCs) marked by Rab5 and Rab7, the lysosome-like Vacuolar Compartment (VAC), and immature secretory organelles (pro-rhoptries and pro-micronemes) (Jimenez-Ruiz *et al*., 2016). Interestingly, in *T. gondii*, proteins acquired from the host cell cytosol are degraded in the VAC during or immediately following invasion and intersect with exocytic trafficking of microneme proteins (Dou *et al*., 2014, McGovern *et al*., 2018). This process is important for

both acute and chronic stages of the infection (Di Cristina *et al*., 2017). Most microneme (for example M2AP, MIC3 and MIC6) and rhoptry proteins (for example ROP1 and ROP13) have N-terminal pro-domains that are cleaved off in a post-Golgi compartment or within the immature secretory organelles (Dogga *et al*., 2017, Miller *et al*., 2003, Soldati *et al*., 1998, Turetzky *et al*., 2010). It has been demonstrated that cathepsin L (CPL), aspartyl protease 3 (ASP3) and subtilisin (SUB2) proteases are responsible for the processing of MIC, ROP and RON proteins, along their trafficking route, from Golgi to mature rhoptries or micronemes (Dogga *et al*., 2017, Parussini *et al*., 2010, Miller *et al*., 2003).

Key trafficking proteins and complexes shown to be required for the biogenesis of dense granules and/or rhoptries and micronemes include: the sortilin-like receptor (SORTLR); the dynamin-related protein B (DrpB); HOPS complex subunits; Rab5A; Rab5C; vacuolar protein sorting 9 (Vps9); syntaxin 6 (Stx6, a parasite SNARE homolog); retromer complex, and the adaptor protein 1 complex (AP1) (Breinich *et al*., 2009, Jackson *et al*., 2013, Kremer *et al*., 2013, Morlon-Guyot *et al*., 2015, Pieperhoff *et al*., 2013, Sakura *et al*., 2016, Sangare *et al*., 2016, Sloves *et al*., 2012, Venugopal *et al*., 2017). Disruption of any of these proteins or complexes leads to parasites deprived of secretory organelles and a mistargeting of GRA, ROP, RON and MIC proteins to the surface of the parasites, vacuolar space, the residual body or to the host cell cytoplasm. These results show that *T. gondii* parasites have repurposed the classical endocytic trafficking regulators of the endolysosomal system to build the parasite secretory organelles and to traffic their contents. However how vesicles containing proteins of the various secretory organelles are sequentially transported, to the different compartments, and how the processes of fusion, fission and membrane recycling occur throughout the miniscule parasite endomembrane system remain enigmatic.

Membranous fusion within the endolysosomal system depends on Rab-GTPases, these mediate the first contact and then membrane-embedded SNAREs drive bilayer fusion (Bonifacino *et al*., 2004, Mima *et al*., 2008, Ostrowicz *et al*., 2008, Ren *et al*., 2009, Sudhof *et al*., 2009). Two tethering complexes termed CORVET (class C core vacuole/endosome tethering) and HOPS (homotypic fusion and vacuole protein sorting) have been described (Nickerson *et al*., 2009, Peplowska *et al*., 2007, Seals *et al*., 2000). These complexes are essential for early-to-late endosome transition, lysosome biogenesis and endolysosomal trafficking pathways (Ostrowicz *et al*., 2010, Solinger *et al*., 2013). Whereas CORVET is associated with early endosomes, HOPS is known to be associated with late endosomes, and lysosomes/vacuole (Spang, 2016). In general, the CORVET and HOPS complexes contain four common subunits (Vps11, Vps18, Vps16 and Vps33) (Fig 1). Studies on different organisms demonstrate these subunits associate with different components. For instance in yeast, the CORVET complex contains two specific subunits called Vps8 and Vps3 whereas in mammalian cells only Vps8 is conserved and Vps3 is replaced by TGFBRAP1 (Fig. 1A) (Balderhaar *et al*., 2013, van der Kant *et al*., 2015). In *Drosophila*, the CORVET complex is composed of only four subunits (Vps16, Vps18, Vps8 and Vps33) (Fig. 1A) (Lorincz *et al*., 2016). In contrast, the composition of the HOPS complex remains the same in yeast and mammals and has only two specific subunits (Vps39 and Vps41) (Fig. 1B) (Balderhaar *et al*., 2013). In mammals, an additional protein called RILP (Rab-Interacting Lysosomal Protein) interacts with Vps11 and Vps41 and make the link between HOPS and Rab7 (Fig. 1B) (van der Kant *et al*., 2015). In the ciliate *Tetrahymena thermophila*, the HOPS specific subunits Vps39 and Vps41 are missing, and most surprisingly the CORVET-specific subunits like Vps8, were amplified to compensate for the lack of the HOPS complex and acquired the unexpected ability to bind to the Rab7 late endosome marker (Fig.1A) (Sparvoli *et al*., 2018). In *Toxoplasma gondii,* an *in silico* search allowed us to identify only the HOPS complex,

whereas the CORVET complex specific subunits Vps3 and Vps8 were absent (Morlon-Guyot *et al*., 2015), suggesting a situation opposite to *Tetrahymena*, a closer organisms within the super-phylum of Alveolates. In *T. gondii*, we showed that removal of the Vps11 subunit affected the biogenesis of the parasite's three secretory organelles (Morlon-Guyot *et al*., 2015). In *T. gondii*, it has been shown that Vps9 is crucial for sorting of proteins destined to secretory organelles (Morlon-Guyot *et al*., 2015, Sakura *et al*., 2016). Vps9 has a guanine nucleotide exchange factor (GEF) activity towards Rab5a, pointing to the existence of a CORVET complex in *Toxoplasma* and prompted us to identify the Vps11 interaction network in this parasite. In this study, we used the GFP-Trap pull-down strategy and uncovered the two HOPS-specific subunits (Vps39 and Vps41) and the four common subunits between CORVET and HOPS (Vps11, Vps18, Vps16 and Vps33). Interestingly, we isolated a protein sharing low similarity to the specific subunit of CORVET (Vps8) and a beach-domain containing protein (BDCP), both playing an essential role within the parasite exocytic pathways. In contrast to Vps8 mutant where a general block in the biogenesis of dense granules, micronemes, rhoptry and VAC compartment was obtained, BDCP shows a more restricted function, and intervenes solely in the biogenesis of both rhoptries and VAC.

Results

Discovery of new sub-units associated to CORVET and HOPS in *T. gondii*

To uncover the components of the CORVET and HOPS in *T. gondii*, we performed GFP-Trap pull-down experiments using anti-GFP antibodies on Vps11-GFP knock-in parasite lysate followed by mass spectrometry identification of the immuno-precipitated proteins (from two independent experiments) (Fig. 2A, supplementary figure 1A, 1B and table 1). An anti-GFP immuno-precipitation on protein extracts from the parental strain expressing the GFP protein alone, was used as control. After several washes, one fifth of each eluate was subjected to SDS-PAGE and silver staining (Fig. 2A). Few proteins bound to GFP or to Vps11-GFP coated beads. Both samples showed a very different profile (Fig. 2A). For mass spectrometry analysis, we selected the proteins identified in both experiments but not in the control strain (Table 1). All the common proteins identified in one of the two experiments and in the negative control, or absent from the control but found in one out of two experiments were excluded (Supplementary table 1). Our results revealed that Vps11 was reproducibly associated with the five other subunits (Vps39, Vps18, Vps16, Vps33 and Vps41) (Table 1) confirming the formation of a conventional HOPS complex in *T. gondii* (Balderhaar *et al*., 2013, Brocker *et al*., 2012). Interestingly, the results revealed > 6 unique peptides that match the amino acid sequence of Vps9 Domain-Containing Protein (Vps9-DCP, a putative Guanine Exchange Factor known to interact with Rab5), but also >10 unique peptides that match a protein (TGME49_289520) with low similarity to the CORVET specific subunit Vps8. TGME49_289520 is a large protein of 3307 amino acids and possesses only conservation with the C-terminal RING domain which, in yeast, functions as a E3 ubiquitin ligase and is believed to regulate the fusion events at the vacuole, most likely through binding interactions with other fusion factors (Supplementary Fig. 2A) (Budhidarmo *et al*., 2012, Hunter *et al*., 2017, Plemel *et al*., 2011). The presence of this Vps8-like protein

suggests that the CORVET complex is present in *Toxoplasma*. We found also 1 to 5 unique peptides that are present in the amino acid sequence of a putative beach domain containing protein (BDCP) conserved in yeast and mammals and described to contribute to membrane fusion and fission events within the lysosomal system. The name "BEACH" domain was originally identified as a conserved region of proteins, whose mutations were responsible of murine disorder (BEige) and human CHediak-Higashi syndrome (Barbosa *et al*., 1996, Nagle *et al*., 1996). Most BDCPs are large proteins and their BEACH domain is located downstream a PH-like domain and upstream one or more WD40 domain(s). In addition to the BEACH domain, *T. gondii* BDCP exhibits also a PH domain and three WD40 motifs (Supplementary Fig. 2A).

Finally one unique peptide in each pull-down was identified for a coccidian hypothetical protein (TGME49_313340). We then assessed the phenotypic scores of the identified proteins (Table 1) (Morlon-Guyot *et al*., 2015, Sidik *et al*., 2016). The scores show that all *Toxoplasma* HOPS- or CORVET-like proteins are essential (Vps39, Vps11, Vps18, Vps16, Vps33, Vps8 and Vps41), whereas Vps9-DCP, BDCP and TGME49_313340 are seemingly important for parasite fitness *in vitro*. Collectively, these data indicate that a functional CORVET and HOPS complexes are present and important in *T. gondii* and that novel uncharacterized proteins might also contribute to the endolysosomal trafficking in *Toxoplasma*.

BDCP and Vps8 are associated to the complex formed by Vps11 and localize to the endomembrane system in *T. gondii*

We identified BDCP and Vps8 as two proteins belonging to the interaction network of the Vps11 protein by mass spectrometry. To validate this data, we carried out a reverse GFP-trap pull-down approach. We first generated double knock-in parasites expressing both, BDCP-

GFP and Vps11-HA_3 or Vps8-GFP and Vps11-HA_3 proteins under the control of their endogenous promoters (Supplementary Fig. 1A and 1B). As negative control, we generated a strain that expresses both the native Vps11-HA_3 and a GFP protein. To verify the interaction between BDCP-GFP or Vps8-GFP and Vps11-HA_3, we performed an immuno-precipitation on double knock-in BDCP-GFP/Vps11-HA_3 or Vps8-GFP/Vps11-HA_3 parasites, using the GFP-Trap pull-down strategy. Subsequent western blot analysis using anti-GFP or anti-HA antibodies revealed the presence of BDCP-GFP, Vps8-GFP and monomeric and dimeric GFP in the eluted fractions (Fig. 2B, left). Importantly, a single band at the appropriate size of Vps11-HA_3 was specifically pulled down with BDCP-GFP and Vps8-GFP but not with GFP alone (Fig. 2B, right). These results confirm the interaction between the Vps11 protein with Vps8 and BDCP.

The association of BDCP and Vps8 with CORVET/HOPS tethering complexes led us to characterize the localization of both GFP-fused proteins with the endogenous Vps11-HA_3 protein and to study their localizations fate in Vps11-depleted parasites (Supplementary Fig. 1C shows the strategy used to fuse the corresponding proteins with 3-HA tags). Anti-GFP antibodies showed a typical endomembrane staining for both BDCP-GFP and Vps8-GFP proteins (Fig. 2C and 2D). As expected, co-localization experiments between the endomembrane protein Vps11-HA_3 and the BDCP-GFP or Vps8-GFP proteins highlighted a significant overlap between both labeling (Fig. 2C and 2D), showing that they are associated with the endomembrane system. Incontrovertibly, the depletion of the Vps11 protein disturbs the localization of both endogenous TgBDCP-HA_3 and TgVps8-HA_3 proteins (Fig. 2E and supplementary Fig. 1C). In the absence of TgVps11, TgBDCP-HA_3 and TgVps8-HA_3 proteins are found dispersed through the parasite cytosol (Fig. 2E). These results indicate that Vps11 is necessary for the efficient association of both BDCP and Vps8 subunits to the endomembrane system of the parasite.

BDCP and Vps8 are associated to a Rab5 sub-compartment

To get more insight into the localization of TgBDCP and TgVps8, we performed co-localization experiments with markers of the secretory pathway. In intracellular parasites, TgBDCP-HA_3 and TgVps8-HA_3 (see supplementary Figs. 1C and 2B for C-terminal HA-tagging and western blot detection of both Vps8 and BDCP proteins) displayed a discrete pattern apical to the nucleus (Fig. 3A and 3B). TgBDCP-HA_3 partially co-localized with the Golgi (NAGT1-RFP), early endosomes (DD-Myc-Rab5B), the pro-ROP4 (immature rhoptries) and the VAC (cathepsin L or CPL) (Fig. 3A and 3C) (Kremer *et al*., 2013, Morlon-Guyot *et al*., 2015, Parussini *et al*., 2010, Pelletier *et al*., 2002). In contrast, TgBDCP-HA_3 did not colocalize with immature micronemes (pro-M2AP), or with late endosomes (DD-Myc-Rab7) (Fig. 3A and 3C) (Kremer *et al*., 2013, Morlon-Guyot *et al*., 2015). Similarly, TgVps8-HA_3 did not co-localize with DD-Myc-Rab7, but strongly concentrates and co-localizes with the DD-Myc-Rab5B marker which occupies a delimited space of the endosome-like compartment (Fig. 3B and 3C) (Kremer *et al*., 2013). In summary, TgBDCP and TgVps8 occupy restricted areas of the parasite endomembrane system and associate with a Rab5-decorated sub-compartment known to assemble with CORVET in most organisms.

***T. gondii* BDCP and Vps8 proteins are essential for parasite survival**

To investigate the functions of TgVps8 and TgBDCP, a conditional knock-down strategy was attempted in the TATi1-ku80ko strain, using the tetracycline-based transactivator system previously developed for *T. gondii* (Supplementary Fig. 3A) (Meissner *et al*., 2001). One clone for each mutant strain was verified by PCR, selected and named Tgbdcpi and Tgvps8i, respectively (Supplementary Fig. 3B). Then, a C-terminal HA_3-tag was inserted by single homologous recombination at the C-terminal end of the gene in the Tgbdcpi and Tgvps8i

strains (Supplementary Fig. 3A), allowing the control of the regulation of the expression after addition of anhydro-tetracycline by IFA and western blot. Both proteins were no longer detectable by IFA and western blot, after 3 days of treatment with ATc (Supplementary Fig. 4), with already marked decrease in BDCPi-HA_3 and Vps8i-HA_3 proteins expression at day 2. The phenotype of TgBDCP or TgVps8 knock-down was first investigated by plaque assays. No plaques were formed by Tgvps8i mutant while only small plaques were visible for Tgbdcpi mutant, (Supplementary Fig. 5), indicating that TgBDCP and TgVps8 are critical for *T. gondii* parasite survival.

Rhoptries and VAC morphologies are altered in TgBDCP-depleted parasites

We next analyze the consequences of the loss of BDCP on the trafficking of different proteins targeted to secretory organelles. We analyzed, the localization of GRA3 (a dense granule marker), pro-ROP4 (an immature rhoptries marker), AMA1, MIC2, 3 and 5 (as markers of micronemes), ARO (a marker of the surface of rhoptries) and finally CPL (a marker of the lumen of the VAC) using specific antibodies (Achbarou *et al*., 1991a, Achbarou *et al*., 1991b, Brydges *et al*., 2006, Lamarque *et al*., 2014). We clearly show that TgBDCP is not involved in the biogenesis of dense granules, pre-rhoptries and micronemes, since markers for these compartments were not affected in absence of the protein (Supplementary Fig. 6). In contrast, immuno-fluorescence analysis of TgBDCP-depleted intracellular tachyzoites, stained with ARO, revealed dramatic changes in rhoptry labeling compared to that of parental tachyzoites (Fig. 4A). Visually the staining of ARO looked abnormal, starting at the apical pole, as in wild-type parasites, but stretches to reach a length positioned below the nucleus of TgBDCP-depleted parasites. The average measurements of the signal showed a doubling in their length (Fig. 4A and 4B). An ultrastructural morphological examination of rhoptries by transmission electron microscopy indicates that

this organelle is not fragmented and does not resemble a series of linked vesicles (Supplementary Fig. 7). To establish whether the rhoptries of TgBDCP-depleted tachyzoites were still capable of secreting ROP1 protein into the host cell, we examined the presence of E-vacuoles (clusters of vesicles containing rhoptry proteins deposited within the host cell cytosol during invasion) and counted their numbers in both the control and in the mutant strains treated with ATc. Our results show a significant decrease in the number of E-vacuoles indicating a defect in rhoptry protein secretion in the Tgbdcpi mutant parasites (Fig. 4C). We next demonstrated that the loss of TgBDCP results in morphological changes of the VAC. We focused on recently invaded parasites in which the VAC in wild-type parasites was visible as a bright dot (Fig. 4D, upper panel). We noted that the VAC seems to have lost its punctate shape as it reveals a more diffuse CPL staining in parasites lacking TgBDCP. This was found in 80% of the parasites in presence of ATc (Fig. 4D, lower panel and 4E). To establish a possible relationship between rhoptries and the parasite vacuolar compartment, we performed colocalization experiments and demonstrated an exclusive partial overlapping between both CPL and ROP7 proteins, in the absence of BDCP protein (Fig. 4F). Altogether, these results suggest that the loss of TgBDCP leads to an enlargement in the morphology of the rhoptries and VAC organelles, most likely impacts their functions and highlight a probable crosstalk between both organelles. Accordingly, we showed that the level of invasion by TgBDCP-depleted parasites was reduced to 20% as compared to control parasites grown in the absence of ATc (Fig. 5A). In contrast, the lack of TgBDCP does not seem to affect gliding motility (Fig. 5B) and exit from infected cells (Fig. 5C). Finally, TgBDCP-depleted parasites showed a modest intracellular growth defect with a moderate increase in the percentage of vacuoles with 2 and 4 parasites and a decrease in those harboring 8 or 16 parasites (Fig. 5D). We then assessed the *in vivo* virulence of mutant tachyzoites of TgBDCP-depleted parasites. Four groups of mice were infected with individual strains (wild-type or

bdcpi ± ATc), each group of 10 mice were intraperitoneally infected with 100 tachyzoites and monitored daily over a period of 45 days. Mice infected with the wild-type tachyzoites died within 10–20 days, in the absence or presence of ATc treatment (Fig. 5E). Similarly, mice injected with bdcpi died between 11 and 15 days, without ATc treatment (Fig. 5E). In contrast, upon treatment with ATc, all the mice survived over the 45 days (Fig. 5E). Altogether, these data imply an important role for TgBDCP in invasion, intracellular growth and virulence processes.

Conditional ablation of TgVps8 disrupts protein trafficking of dense granules, rhoptries, a subset of micronemes and VAC.

We then examined the phenotypic consequences of TgVps8 loss on the subcellular localizations of different secretory organelle markers. In ATc-induced Tgvps8i mutants, the dense granules GRA3, GRA16 and GRA24 proteins were abnormally sorted into the host cytoplasm (black asterisk) as compared to their localization with the PV space in the control strain (Fig. 6A and supplementary Fig. 8A). Similarly, in TgVps8-depleted parasites, the pro-rhoptry marker pro-ROP4, ROP13, ROP1 and RON2 were detected at unusual locations such as the residual body (yellow asterisk) or the host cell cytoplasm (black asterisk) compared to their typical localizations (proximal to parasite nuclei for pro-rhoptry or at the apex for ROPs and RONs) in ATc-treated control parasites (Fig. 6A and supplementary Fig. 8B). Next, we analyzed by IFA two different pro-micronemal proteins. Surprisingly, we noticed conflicting consequences in the trafficking pathways towards pro-micronemes. The location of pro-M2AP is not affected while pro-MIC3 accumulates in the residual body (Fig. 6A and supplementary Fig. 8C). Then, by studying a panoply of micronemal proteins, we noticed three categories of atypical localizations of these proteins in the Tgvps8i mutant parasites. In one category, MIC3 (Fig. 6A), MIC5, M2AP, MIC1, MIC4, MIC10 and PLP1

(Supplementary Fig. 8D) were unusually found in the cytoplasm of the host cell. In another category, MIC8 (Fig. 6A), GAMA and SUB1 (Supplementary Fig. 8E) were mislocalized and found associated with the parasite pellicle. Finally, MIC6, MIC2 and AMA1 were detected exclusively at the extreme apex of the parasite (Fig. 6A and supplementary Fig. 8F). Altogether, these data clearly indicate that TgVps8 is required for correct proteins trafficking, sorting and delivery to the three main secretory organelles: rhoptry, micronemes and dense granules (Fig. 6B). In addition, our data may suggest that TgVps8 is required for the transport of a subset of pre-microneme and microneme proteins (Fig. 6B). The correct routing of pro-M2AP towards pro-micronemes and the trafficking of MIC6, MIC2 and AMA1 located at the extreme apical end of TgVps8-depleted parasites raises questions regarding the sub-compartmentalization of pro-micronemes and the existence of different transport pathways for a subset of microneme proteins (Fig. 6B).

Finally, we demonstrated that the loss of TgVps8 disturbs the punctate staining of CPL protein localized within the lumen of the VAC compartment (Fig. 7A, compare upper and lower panels). In TgVps8-depleted parasites, we noticed a widely diffuse CPL staining that could indicate morphological changes in the VAC compartment. This characteristic was present in 80% of the mutant parasites treated in presence of ATc (Fig. 7B).

TgVps8 silencing abolishes host cell infection by *T. gondii*.

To scrutinize the effect of TgVps8 depletion on specific stages of the lytic cycle, we investigated invasion, gliding motility, replication, and egress of parasites. TgVps8-depleted parasites were drastically impaired in invasion, with 0% capacity to invade as compared with control strain (Fig. 7C). Moreover, TgVps8-depleted parasites were unable to glide presumably due to their limited number of micronemes and their powerlessness to secrete adhesins (Fig. 7D and 7E). Next, by performing intracellular growth assays, we noticed that

Vps8-depleted parasites showed an important growth defect, as shown by the accumulation of vacuoles containing mainly 1, 2 or 4 parasites only (Fig. 7F). We also observed an important defect in egress as ~40% of vacuoles were lysed upon induction of infected cells by the calcium ionophore A23187 (Fig. 7G). We further extended our analysis and examined the role of TgVps8 *in vivo*. Mice were infected with vps8i or its parental strain with or without ATc treatment. Consistently with all the *in vitro* defects we obtained upon depletion of TgVps8, ATc-treated mice inoculated with Tgvps8i displayed 100% survival rates as compared to ATc-untreated mice which succumbed to the infection by day 15 (Fig. 5E). Mice infected with the parental strain succumbed to the infection regardless of the initiation of ATc treatment (Fig. 5E). Thus, the conditional ablation of TgVps8 abolished *T. gondii* virulence in mice. Altogether, phenotypic data demonstrate that functional Vps8 is essential for secretory organelle biogenesis, gliding motility, host cell invasion and contributes to parasite growth and egress *in vitro*, and knocking-down TgVps8 abolishes parasite virulence *in vivo*.

TgVps8 is required for the accurate targeting of other Vps proteins belonging to CORVET/HOPS, dictates the targeting of TgASP3 maturase and the putative casein kinase 3 like.

We wanted to examine whether the loss of TgVps8 affects the association of the different factors involved in the biogenesis of secretory organelles to the endomembrane system of the parasite. HA- or GFP-tagged versions for TgVps11 (CORVET-HOPS core complex), TgVps39 (a canonical HOPS subunit), TgVps18 (CORVET-HOPS core complex), TgCHC (trans-Golgi marker), TgAP1 (belongs to the network of interaction of Vps10), TgMon1 (Rab7 interactor), TgVps9 (interacts with TgRab5a), TgVps35 (a member of the retromer complex), TgASP3 (associates with the endosomal system) and also TgCK3L (mediates phosphorylation of the HOPS subunit Vps41 in yeast) were generated (Supplementary Fig.

1A and 1C). We also transiently expressed an additional DD-Myc-tagged copy of each Rab for the Rab-GTPases TgRab7, TgRab5A, B, and C. In the presence of TgVps8, all these proteins displayed a patchy or a Golgi endosomal-like staining near the apical area of the nucleus (Fig. 8A and Supplementary Fig. 9). Interestingly, upon treatment with ATc, the apically defined localizations to nuclei of TgVps11, TgVps39, TgVps18, TgCHC, TgASP3 and TgCK3L were partially or completely abolished (Fig. 8A). Instead, only a cytoplasmic signal (TgVps11, TgVps39, TgVps18 and TgCK3L) or a residual body labeling (TgASP3, white asterisk) or fragmented staining (TgCHC) of these proteins was observed in the absence of TgVps8 (Fig. 8A). The defined labelling for TgAP1, TgMon1, TgRab5A, B and C, TgRab7, TgVps9 and TgVps35 was maintained (Supplementary Fig. 9). Taken together, these data suggest that TgVps8 protein interacts with some proteins found in the CORVET/HOPS complexes and may maintain the integrity of the trans-Golgi network associated to the clathrin-heavy chain protein.

Discussion

Apicomplexan parasites produce unique secretory organelles (dense granules, rhoptries and micronemes) containing virulence factors, which are essential for their ability to invade and manipulate the host cell (Bougdour *et al*., 2014, Hakimi *et al*., 2015, Hakimi *et al*., 2017, Kemp *et al*., 2013, Liu *et al*., 2017, Mercier *et al*., 2015). Consequently, the conveyance of virulence factors localized in these secretory organelles has been thoroughly investigated (Jimenez-Ruiz *et al*., 2016). However, the molecular basis implicated in their biogenesis and maintenance is not fully understood. Various studies highlighted the presence of an endosomal-like pathway for secretory organelle biogenesis in *T. gondii* (Jimenez-Ruiz *et al*., 2016). In this context, we have already characterized the HOPS tethering complex as key player in the biogenesis of secretory organelles (Morlon-Guyot *et al*., 2015). Our inability to identify *in silico* the specific subunits of CORVET, prompted us to perform a proteomic study using Vps11, a common member of CORVET and HOPS, as bait to solve the enigma related to the absence of CORVET complex in *Toxoplasma*. Using parasites harboring TgVps11-GFP and pull-down analyses, we uncovered both several canonical components of CORVET/HOPS complexes, and also uncharacterized proteins that are conserved in eukaryotes or unique to apicomplexans (Table 1). Among these, TgBDCP and TgVps8 belong to the interaction network of TgVps11 (a common subunit to both CORVET and HOPS complexes). Conditional depletion of TgBDCP revealed its role in invasion and to a lesser extent in growth. Interestingly, in TgBDCP-depleted parasites, rhoptries appear to undergo morphological aberrations (ARO length staining ~2 times longer than normal rhoptries labeling). The vacuolar compartment (VAC) also seems enlarged. Depletion of TgBDCP abolishes the *in vivo* virulence of the parasite. Altogether, our results show that TgBDCP is crucial for maintaining the biogenesis of *Toxoplasma* rhoptries and VAC, for host cell invasion, optimal growth and virulence. The defect in invasion may be due to

morphologically aberrant rhoptries affecting the secretion of their contents in the mutant. The defect in optimal growth may result from the aberrant VAC enlargement, which may affect the degradation of nutrients that are normally captured by this parasite compartment and are essential for its growth (Di Cristina *et al*., 2017, Dou *et al*., 2014, McGovern *et al*., 2018), and/or defect of release of rhoptry proteins that might contribute to intracellular growth. Surprisingly, we observed no obvious impact on pro-rhoptries, suggesting that TgBDCP functions downstream of pro-rhoptries formation in a precise step of the vesicular trafficking pathway involving CORVET and HOPS tethering complexes. In parasites that do not express BDCP, labeling rhoptries with ARO surface protein resembles the effect seen in parasites that express ARO protein lacking its sixth armadillo repeat (Mueller *et al*., 2016). The phenotype observed had been interpreted as an inappropriate recycling of mature rhoptry membranes originating from the mother cell during the formation of daughter cells. Given the involvement of BEACH domain containing proteins in membrane recycling processes in other organisms (Cullinane *et al*., 2013), it is tempting to speculate that BDCP may play a role in the recycling of mature rhoptries during endodyogeny in *T. gondii*. This hypothesis awaits further experimentation validation. Nevertheless, our results may suggest a novel uncharacterized trafficking pathway between mature rhoptries and other sub-compartments of the parasite endolysosomal system. This new trafficking pathway may involve transport between the VAC and the mature rhoptries. It is still underexplored whether the rhoptry proteins like few described micronemal proteins traffic through the VAC before being transported to the mature rhoptries (Parussini *et al*., 2010). Further investigations are required to establish whether rhoptry biogenesis is affected because of the impact on the VAC in TgBDCP-depleted cells. This would establish a novel and uncharacterized crosstalk between the parasite vacuolar compartment and rhoptries. If so, this would support a model in which

TgBDCP is required for rhoptry biogenesis from the VAC or is necessary for preventing inappropriate trafficking of ROPs proteins to the parasite VAC.

In other organisms, the biogenesis, morphology and activity of lysosome-related organelles (LROs) relies on important factors such as BEACH domain containing proteins (BDCPs). Point mutations specific to the BEACH domain contained in nine human proteins, the BDCPs, are responsible for rare and serious human diseases (Barbosa *et al*., 1996, Nagle *et al*., 1996). Patients suffering from these diseases exhibit enlarged LROs with impaired function in their cells. To date, no binding partner has been identified for BDCPs. Thus, it is currently entirely unresolved how BDCPs affect LROs size and function. LROs are a group of functionally diverse compartments that share features with lysosomes but have distinct morphology, composition and/or functions and harbor specific cargoes that confer them unique properties (Raposo *et al*., 2007). LROs are accessible to endocytic traffic, their contents derive from the endosomal system, and they contain lysosomal proteins such as proteases and a low luminal pH (Raposo *et al*., 2007). Like other LROs, rhoptries and VAC are formed *via* endosomal trafficking, contain proteases and their respective lumens are probably acidic (Dou *et al*., 2013, Hajagos *et al*., 2012, Lentini *et al*., 2017, Miller *et al*., 2003, Morlon-Guyot *et al*., 2015, Shaw *et al*., 1998). Interestingly, we demonstrate for the first time that a BDCP protein belongs to the network of interaction of CORVET and HOPS tethering complexes. The interaction of BDCP with CORVET and HOPS, which we have identified in *Toxoplasma,* now provides an important new angle, providing perspectives for addressing the role of other eukaryotic BDCPs in the endolysosomal system.

The Vps11-interacting network also includes Vps8, a CORVET-specific subunit. We then showed that TgVps8 localizes to the Rab5-subcompartment and physically interacts with the core CORVET/HOPS complexes. Genetic ablation of TgVps8 demonstrates that its function is essential for the biogenesis of micronemes, dense granules, rhoptries and the VAC

compartment. As a consequence vps8i mutant parasites were completely paralyzed for gliding motility and host cell invasion. Not surprisingly, depletion of TgVps8 resulted in a lethal phenotype in mice. Interestingly, while the routing of most of the MICs tested was completely altered, the targeting of AMA1, MIC2 and MIC6 was only partially affected. These subset of micronemes proteins were still detected at the very apical end of the parasites, providing further evidence of the presence of at least two different populations of micronemes and/or two distinct trafficking pathways for micronemal proteins. Indeed, micronemal organelles are organized in distinct sub-compartments and only some microneme proteins require Rab5A and Rab5C for their routing towards one of the two microneme subsets (Kremer *et al*., 2013). Our results demonstrated that targeting of pro-MIC3 is compromised in TgVps8-depleted parasites, while in contrast the targeting of pro-M2AP remains intact. Very little is known about pro-micronemes but our observations suggest that there are different sub-compartments of pro-micronemes and might suggest differential pathways of trafficking to mature micronemes (this study and (Morlon-Guyot *et al*., 2015). Further investigations are now required to address this hypothesis in more details.

The VAC compartment seems to be enlarged in absence of TgVps8. This might be due to an accumulation of undigested material within the VAC compartment that results from lack of VAC acidification, and/or a deficiency in membrane recycling. In yeast, a role of Vps8 in vacuole acidification has been proposed (Horazdovsky *et al*., 1996). Vps8 is assigned to the class D vps mutant group because cells that completely lack Vps8 exhibit a single enlarged vacuole that is not properly acidified. In the same line, cells deficient in Vps3 (the other subunit specific to CORVET) were unable to generate a pH gradient across the vacuolar membrane, and they failed to assemble peripheral membrane subunits of the V-ATPase onto the cytoplasmic surface of the vacuole (Raymond *et al*., 1992).

Furthermore, we demonstrated that the endosomal accumulation of other subunits that are either HOPS specific (Vps39), common to CORVET and HOPS (Vps18 and Vps11) or interacting with HOPS (CHC and CK3L) are severely compromised in Tgvps8 mutants. Consistent with this, it has been shown that Vps8 binds through both the RING domain and a disordered C-terminus to both Vps18 and Vps11 subunits (Hunter *et al*., 2017). Our hypothesis is that TgVps8, in addition to acting as a sorting factor for ROP/MIC proteins, delivers proteases (such as ASP3), which are involved in the processing of pro-proteins, to secretory organelles. Finally, in TgVps8-depleted cells, the atypical distribution of the clathrin heavy chain (CHC) is not surprising since an interaction between the HOPS complex and the clathrin/AP-3 complexes has been previously described (Zlatic *et al*., 2011). Despite the demonstration of a direct interaction between Vps8 and Rab5, we did not notice a modification in the localizations of the three Rab5s of the parasite (Rab5A, Rab5B and Rab5C) (Markgraf *et al*., 2009). Consistently, CORVET localization requires the Rab5 homologs Vps21 and Ypt52, whereas Rab5 localization is caspase-dependent (Cabrera *et al*., 2013, Torres *et al*., 2008).

We failed to identify CORVET/HOPS accessory proteins such as Rab-GTPases, GEF and SNAREs in the immuno-precipitates of *T. gondii* using Vps11 as a bait. This observation suggests that additional pull-down experiments may be required using other subunits such as Vps8, Vps41, Vps39 and Vps33 as an alternative solution to identify the missing members of CORVET and HOPS complexes in *Toxoplasma*. In addition, our proteomic analysis revealed the absence of the CORVET-specific subunit Vps3. Interestingly, BlastP analysis revealed that TGFBRAP1 is present in *T. gondii* genome and appears to be essential according to the negative score attributed to this protein (Sidik *et al*., 2016). It remains important to investigate if TgTGFBRAP1 is associated with the CORVET complex and if it is involved in the biogenesis of secretory organelles. Overall, our recent findings may suggest that the

CORVET complex are composed differently in *Toxoplasma* and probably in other apicomplexan parasites, and has been adapted to accommodate the complexity of trafficking pathways in these parasites towards their unique secretory organelles (Fig. 9B). In conclusion, our data: 1- support previous results demonstrating that the endosomal system is adapted for secretory organelle biogenesis and discharge of factors required for the intracellular lifestyle of the parasite *T. gondii* and 2- contribute to the emerging view that multi-subunit tethering complexes are dynamic in composition in order to facilitate multiple transport pathways.

Experimental procedures

Parasite culture

Toxoplasma gondii RH strains RH-ku80ko (Huynh *et al*., 2009) and TATi1-ku80ko (Sheiner *et al*., 2011) were grown in HFFs maintained in Dulbecco's modified Eagle's medium (DMEM; GIBCO, Invitrogen) supplemented with 5% fetal calf serum (FCS) and 2 mM glutamine. Selections of transgenic parasites were performed with chloramphenicol for CAT selection (Kim *et al*., 1993), pyrimethamine for DHFR-TS selection (Donald *et al*., 1993), 1 µM Shld-1 for DD fusion stabilization (Herm-Gotz *et al*., 2007) and ATc at 1.5 µg/ml for the inducible system (Meissner *et al*., 2001).

***Toxoplasma* vectors and generation of transgenic *T. gondii* parasites.**

Primers used in this study are listed in Table S2. Plasmids LIC-CAT-Vps11/Ctg-GFP, LIC-CAT-BDCP/Ctg-GFP, LIC-CAT-Vps8/Ctg-GFP, LIC-CAT-AP1/Ctg-GFP, LIC-CAT-CHC/Ctg-GFP, LIC-DHFR-Vps11/Ctg-HA_3, LIC-CAT-Vps8/Ctg-HA_3, LIC-CAT-GRA16/Ctg-HA_3, LIC-CAT-GRA24/Ctg-HA_3, LIC-CAT-ROP13/Ctg-HA_3, LIC-CAT-M2AP/Ctg-HA_3, LIC-CAT-MON1/Ctg-HA_3, LIC-CAT-Vps9/Ctg-HA_3, LIC-CAT-Vps35/Ctg-HA_3, LIC-CAT-Vps18/Ctg-HA_3, LIC-CAT-Vps39/Ctg-HA_3, LIC-CAT-Vps11/Ctg-HA_3, LIC-CAT-MIC8/Ctg-HA_3, LIC-CAT-BDCP/Ctg-HA_3, LIC-CAT-ASP3/Ctg-HA_3 and LIC-CAT-CK3L/Ctg-GFP were designed to add a sequence coding for a GFP or (3)HA at the endogenous locus of TgVps11, TgBDCP, TgVps8, TgAP1, TgCHC, TgGRA16, TgGRA24, TgROP13, TgM2AP, TgMON1, TgVps9, TgVps35, TgVps18, TgVps39, TgMIC8, TgASP3 and TgCK3L open reading frames. A 1216, 1171, 1119, 1045, 989, 1182, 881, 1063, 1197, 1302, 1481, 1306, 1246, 1574, 1193, 1201 and 1184 bp fragment corresponding to the 3′ of TgVps11, TgBDCP, TgVps8, TgAP1, TgCHC, TgGRA16, TgGRA24, TgROP13, TgM2AP, TgMON1, TgVps9, TgVps35, TgVps18, TgVps39, TgMIC8, TgASP3 and TgCK3L, respectively, were amplified from genomic DNA using primers listed in Table S2 and cloned into LIC-CAT-GFP or LIC-DHFR-HA_3 or LIC-CAT-HA_3 vectors (Huynh *et al*., 2009). 40 µg of these plasmids was digested by the restriction enzymes cited in supplementary figure 1 and then transfected in the RH-ku80ko or bdcpi or vps8i strains and were subjected to chloramphenicol or pyrimethamine selections.

A 1282 and 1302 bp fragment corresponding to the 5′ of the TgBDCP or TgVps8 coding region (downstream of the codon corresponding to the first predicted in-frame methionine residue) was amplified by PCR from *T. gondii* genomic DNA and then cloned in the DHFR-tetO7-Sag4 plasmid between BglII and NotI restriction sites (Morlon-Guyot *et al*., 2014, Sheiner *et al*., 2011) downstream the DHFR selection marker, tetO7 tet operator and pSag4

promoter. These constructs were linearized by SfoI and AatII respectively prior to transfection. Transfected TATi1-ku80ko parasites were selected with pyrimethamine and cloned by limit dilution. Positive clones were verified by PCR to detect the native locus or the single homologous recombination of the inducible vectors in the BDCP and Vps8 loci.

To detect the Golgi and the ELC, the bdcp-HA_3 or vps8-HA_3 or vps8i strains were transfected transiently with 100 µg of NAGT1-RFP or DD-Myc-Rab5A or DD-Myc-Rab5B or DD-Myc-Rab5C or DD-Myc-Rab7 circular vectors, respectively (Kremer *et al*., 2013, Nishi *et al*., 2008, Pelletier *et al*., 2002).

Protein detection by Western blot

To detect BDCP-HA_3, BDCPi-HA_3, BDCP-GFP, Vps8-HA_3, Vps8i-HA_3, Vps8-GFP, GFP, Vps11-HA_3 or MIC2 or ROP5, PRF, GRA3 proteins, parasite lysates or eluted proteins were separated on 3-8%, 10% or 12% acrylamide gels depending on their size prior to detection. Upon transfer to nitrocellulose membranes, the blots were probed with appropriate antibodies in 5% non-fat milk powder in TNT buffer (50 mM Tris pH 8; 150 mM NaCl; 0.05% Tween-20) (EUROMEDEX). The primary antibodies used and their respective dilutions were rat anti-HA (Roche) at 1/300, rabbit anti-GFP (abcam) at 1/1000, mouse anti-ROP5 at 1/100, rabbit anti-PRF at 1/1000, mouse anti-MIC2 at 1/100 and mouse anti-GRA3 at 1/1000. Bound secondary conjugated antibodies were visualized using either the ECL system (Amersham Corp.) or using alkaline phosphatase kit according to manufacturer's instructions (Promega).

Fluorescent staining of cells

Briefly, for IFAs of intracellular parasites, infected confluent HFF monolayers were fixed for 20 min in 4% paraformaldehyde in phosphate buffered saline (PBS) or with cold methanol for 6 min, permeabilized with 0.2% tritonX-100, blocked with 10% FCS in PBS and then incubated with primary antibodies [anti-HA (Roche) 1:100, anti-GFP (abcam) 1:2000, anti-Myc 1:100 (Santa Cruz Biotechnology), anti-SAG1 1:1000 (Couvreur *et al*., 1988), anti-MIC3 1:500 (Achbarou *et al*., 1991a), anti-proMIC3 1:200 (Cerede *et al*., 2002), anti-ROP1 1:1000 (Leriche *et al*., 1991), anti-ROP7 1 :1000 (kindly provided by Dr Peter Bradley), anti-AMA1 1:1000 (Lamarque *et al*., 2014), anti-GRA3 1:500 (Achbarou *et al*., 1991b), anti-CPL 1:500 (Larson *et al*., 2009), anti-proM2AP 1:400 (kindly provided by Dr Vern Carruthers), anti-proROP4 1:100 (kindly provided by Dr Gary Ward), anti-MIC2 1:400 (Achbarou *et al*., 1991a), anti-RON2 1:500 (Besteiro *et al*., 2009), anti-GAP45 1:2000 (Frenal *et al*., 2010), anti-GAMA 1:500 (Huynh *et al*., 2016), anti-MIC5 1:500 (Brydges *et al*., 2006), anti-MIC6 1:1000 (Reiss *et al*., 2001), anti-MIC10 1:500 (Hoane *et al*., 2003), anti-PLP1 1:500 (Kafsack *et al*., 2009), anti-MIC1 1:500 (Reiss *et al*., 2001), anti-MIC4 1:1000 (Reiss *et al*., 2001), anti-SUB1 1:500 (Miller *et al*., 2001), anti-ARO 1:1000 (Mueller *et al*., 2013)], followed by goat anti-rabbit or goat anti-mouse or goat anti-rat immunoglobulin G conjugated to Alexa Fluor 488 or Alexa Fluor 594 (Molecular Probes, Invitrogen). Coverslips were mounted onto microscope slides using Immumount (Calbiochem). Samples were observed with a Zeiss Axioimager epifluorescence microscope equipped with an apotome and a Zeiss Axiocam MRmCCD camera driven by the Axio vision software (Zeiss) at the Montpellier RIO imaging facility.

Plaque assay

Fresh monolayers of HFF on circular coverslips were infected with parasites in the presence or absence of 1.5 μg/ml ATc for 7days. Fixation, staining and visualization were performed as previously described (Daher *et al*., 2010).

Intracellular growth assays

Parasites (bdcpi, vps8i) were pretreated for 48 hrs or 40 hrs respectively, with or without 1.5 μg/ml ATc, collected promptly after egress and inoculated onto new HFF monolayers in the presence of ATc during 24 hrs for bdcpi or 32 hrs for vps8i. The infected host cells with different strains were then fixed with PFA and stained with anti-TgGAP45 antibodies. The numbers of parasites per vacuole were counted for more than 300 vacuoles for each condition. Data are mean values ± standard deviation (S.D.) from three independent biological experiments.

Invasion assays

Parasites were treated in total for 72 hrs with or without 1.5 μg/ml ATc, and collected promptly after egress. For invasion assays, 5×10^6 freshly released tachyzoites were sedimented on confluent cells at 4°C for 30 min on ice and warmed up for invasion during 5 min at 38.5°C. Invasion was stopped by fixation in 4% PAF and parasites were further processed for IFA. Prior to triton permeabilization, extracellular parasites were labelled with anti-SAG1 antibodies, while following permeabilization, intracellular parasites were stained with anti-ROP1 antibodies that labelled the nascent PV (Lebrun *et al*., 2005). Data are mean values ± SD from three independent biological experiments. For each condition, 300 parasites were observed.

Egress assay

Parasites were pretreated for 39 h with or without 1.5 µg/ml ATc collected promptly after egress and inoculated onto new HFF monolayers in the presence of ATc during 33 hrs. After 33 hrs of intracellular growth, media were changed and incubated for 5 min at 37°C with DMEM containing 0.06% of DMSO or 3 µM of the Ca^{2+} ionophore A23187 (from Streptomyces chartreusensis, Calbiochem 100105) as previously described (Daher *et al*., 2010). Data are mean values ± SD from three independent biological experiments. For each condition, 300 parasites were observed.

Gliding motility assay

Parasites were treated in total for 72 hrs with or without 1.5 µg/ml ATc, and collected promptly after egress. Freshly released tachyzoites were collected by centrifugation, resuspended in 100 µl and deposited onto poly-L-lysine coated coverslips (1 mg/ml, 2 hrs at room temperature) in a wet environment for 15 min at 37°C. Parasites were fixed with PAF/GA and IFA using the anti-SAG1 antibody was performed to visualize the trails.

Ethics statement and *in vivo* experiments

All mice protocols were approved by the Institutional Animal Care and Utilization Committee (IACUC) of the American University of Beirut (AUB) (IACUC Permit Number no.14-3-278). All animals were housed in approved pathogen-free housing. Human endpoints were used as requested by the AUB IACUC according to Association for Assessment and Accreditation of Laboratory Animal Care International guidelines and guide of animal care use book (Guide, NRC 2011). Mice were sacrificed for any of the following reasons: (i) impaired mobility (the inability to reach food and water); (ii) inability to remain upright; (iii) clinical dehydration and/or prolonged decreased food intake; (iv) weight loss of 15–20%; (v)

self-mutilation; (vi) lack of grooming behavior/rough/unkempt hair coat for more than 48 hrs; (vii) significant abdominal distension; and (viii) unconsciousness with no response to external stimuli. Mice were deeply anaesthetized with isoflurane before cervical dislocation. Ten-week-old Balb-c mice (Charles River, France) were infected by i.p. injection of 100 tachyzoites freshly harvested from cell culture. Invasiveness of the parasites was evaluated by simultaneous plaque assay of a similar dose of parasites on human foreskin fibroblasts (HFFs). Mouse survival was monitored daily during 45 days, end-point of all experiments. The immune response of surviving animals was tested following eye pricks performed on day 7 post infection. Sera were tested by western blotting against tachyzoite lysates. Data were represented as Kaplan and Meier plots using Excel.

Identification of TgVps11 partners

Freshly released tachyzoites (around 10^9 freshly egressed parasites) were harvested, washed in PBS, and lysed in RIPA buffer (50 mM Tris HCl pH 7.4, 1% NP40, 76 mM NaCl, 2 mM EGTA, 10% Glycerol, protease inhibitor cocktail [Roche]) and incubated on ice for 20 minutes. After centrifugation at 14,000 rpm during 45 minutes at 4°C, the supernatants were subjected to immuno-precipitation using anti-GFP lama antibodies (GFP-Trap Agarose Beads from ChromoTek). Following stringent washing conditions (50 mM Tris HCl pH 7.4, 1% Nonidet P-40, 76 mM NaCl, 2 mM EGTA, 10% Glycerol, protease inhibitor cocktail [Roche]), one fifth of the beads for each condition were suspended in loading buffer for SDS-PAGE, and the proteins were then separated on a 4–12% gradient gel and detected by silver staining. The remaining beads were directly submitted to trypsin treatment for mass spectrometry analysis. Pull-down experiments have been repeated two times with different batches of parasites.

Mass-spectrometry proteomic analysis

GFP-Trap agarose beads and associated proteins were subjected to trypsin digest using the FASP protocol (Wisniewski *et al*., 2009). The resulting tryptic peptides were solubilized in 2% acetonitrile with 0.1% TFA and fractionated on a nanoflow uHPLC system (Thermo Scientific RSLCnano). Peptides were desalted and concentrated for 4 min on a C18 trap column, running with 2% acetonitrile, 0.1% (v/v) TFA at 25 µl/min, then fractionated on a C18 PepMap analytical column at a flow rate of 0.3 µl/min. Peptide fractionation was achieved using an acetonitrile gradient comprising 3.2 - 32% v/v over 4 - 27 min, 32% - 80% v/v over 27 - 36 min, 80% v/v 36- 41 min and re-equilibrium at 3.2%) for a total time of 45 min and maintaining 0.1% v/v formic acid throughout. Eluate was delivered by electrospray into an LTQ Velos Orbitrap mass spectrometer (Thermo Scientific). Mass spectrometric (MS) analysis were performed using a continuous duty cycle of survey MS scan followed by up to ten MS/MS analyses of the most abundant peptides, choosing the most intense multiply charged ions with dynamic exclusion for 120s. The resulting data were used as input to MASCOT MS/MS Ion search of the *Toxoplasma* genome dataset obtained from TOXODB, using the Matrix Science. Mass tolerance was set at 10 ppm for MS data and 0.5 Da for MS/MS data.

Microneme secretion assay

Freshly egressed parasites were re-suspended in equal volume of intra-cellular (IC) buffer (5 mM NaCl, 142 mM KCl, 1 mM $MgCl_2$, 2 mM EGTA, 5.6 mM glucose, 25 mM HEPES, pH 7.2) prior to pelleting (1,050 rpm/10 min). Pellets were subsequently washed in IC buffer and re-pelleted before resuspension in serum-free medium and 500 mM propranolol (37°C/30 min). Parasites were pelleted (1,000 × g/5 min/4°C), and supernatant was transferred to new Eppendorf tubes and re-pelleted (2,000 × g/5min/4°C). Final supernatant (excreted secreted

antigens [ESAs]) was re-suspended in sample buffer (50 mM Tris-HCl [pH 6.8], 10% glycerol, 2 mM EDTA, 2% SDS, 0.05% bromophenol blue, 100 mM DTT) and boiled prior to analysis by immunoblotting using anti-MIC2 and anti-GRA3 antibodies.

Analysis of CPL labelling and ARO length staining

Wild-type (TATi1-ku80ko), bdcpi and vps8i parasites were treated with 1.5 μg/ml ATc for 2 and 3 days respectively. Freshly lysed parasites were added to HFF cells, allowed to settle for 15 min at room temperature, and then incubated at 37°C for 1 h for invasion. Non invaded parasites were washed away with phosphate-buffered saline. Infected HFF cells were fixed with 4% paraformaldehyde and stained with rabbit anti-TgCPL antibodies. Images were captured with a Zeiss Axio-imager epifluorescence microscope equipped with a Zeiss AxioCam MRm camera. The intact or dispersed CPL staining was quantified using Zeiss Axiovision software.

For ARO staining, images were acquired by focusing on the ARO signal in the maximum number of parasites within a field of view and captured on a Zeiss Axio-imager epifluorescence microscope equipped with a ×100 oil objective and an AxioCAM MRm camera and processed using Zeiss Axiovision software. ARO length staining measurements were only performed on rhoptries that were within focus using ImageJ program. Equal parameters for the capture and enumeration of images were consistently applied to all samples. Hundreds of ARO labeling (potentially representing the surface of rhoptries) per condition were analyzed before plotting the graph presented in figure 4B.

Electron Microscopy

Infected HFF monolayers on coverslips were fixed for 4 hours at room temperature with 2.5% glutaraldehyde (EMS) in 0.1M phosphate buffer pH7.2, washed in buffer and post-fixed for 1 hour in 1% OsO4, washed in water and stained overnight in 2% uranylacetate. Coverslips were then dehydrated in ethanol series and embedded in Epon (Embed 812, EMS). Ultrathin sections were prepared with a Leica ultracut E microtome, contrasted with 2% uranylacetate in ethanol and lead citrate and observed with a JEOL 1200E electron microscope.

Statistics

P values were calculated in Excel using the Student's t-test assuming equal variance, unpaired samples, and using two tailed distribution. Means and SD were also calculated in Excel.

Acknowledgements

We wish to thank Dominique Soldati-Favre, Vern Carruthers, Jean-François Dubremetz, Ke Hu, Gary Ward, Lilach Sheiner and David Roos for their kind gift of cell lines, plasmids or antibodies. We also thank the "Montpellier Ressources imagerie" platform for providing access to their microscopes. This work was made possible through core support from the Fondation pour la Recherche Médicale (Equipe FRMDEQ20130326508), the Labex Parafrap (ANR-11-LABX-0024), the Medical Practice Plan (Faculty of Medicine, American University of Beirut), the Centre National de Recherche Scientique Libanais (CNRS-L) and the AUB-CNRS-L GRP funding. Markus Meissner was supported by an ERC Starting grant, (ERC-2012-StG 309255), and a Wellcome Senior Fellowship, 087582/Z/08/Z.

The authors declare that there are no conflict of interest.

References

Achbarou, A., Mercereau-Puijalon, O., Autheman, J.M., Fortier, B., Camus, D. and Dubremetz, J.F. (1991a). Characterization of microneme proteins of *Toxoplasma gondii*. *Mol Biochem Parasitol* **47,** 223-233.

Achbarou, A., Mercereau-Puijalon, O., Sadak, A., Fortier, B., Leriche, M.A., Camus, D. and Dubremetz, J.F. (1991b). Differential targeting of dense granule proteins in the parasitophorous vacuole of *Toxoplasma gondii*. *Parasitology* **103,** 321-329.

Balderhaar, H.J. and Ungermann, C. (2013). CORVET and HOPS tethering complexes - coordinators of endosome and lysosome fusion. *J Cell Sci* **126,** 1307-1316.

Barbosa, M.D., Nguyen, Q.A., Tchernev, V.T., Ashley, J.A., Detter, J.C., Blaydes, S.M., *et al*. (1996). Identification of the homologous beige and Chediak-Higashi syndrome genes. *Nature* **382,** 262-265.

Besteiro, S., Michelin, A., Poncet, J., Dubremetz, J.F. and Lebrun, M. (2009). Export of a *Toxoplasma gondii* rhoptry neck protein complex at the host cell membrane to form the moving junction during invasion. *PLoS Pathog* **5,** e1000309.

Blader, I.J. and Koshy, A.A. (2014). *Toxoplasma gondii* development of its replicative niche: in its host cell and beyond. *Eukaryot Cell* **13,** 965-976.

Bonifacino, J.S. and Glick, B.S. (2004). The mechanisms of vesicle budding and fusion. *Cell* **116,** 153-166.

Bougdour, A., Tardieux, I. and Hakimi, M.A. (2014). *Toxoplasma* exports dense granule proteins beyond the vacuole to the host cell nucleus and rewires the host genome expression. *Cell Microbiol* **16,** 334-343.

Breinich, M.S., Ferguson, D.J., Foth, B.J., van Dooren, G.G., Lebrun, M., Quon, D.V., *et al*. (2009). A dynamin is required for the biogenesis of secretory organelles in *Toxoplasma gondii*. *Curr Biol* **19,** 277-286.

Brocker, C., Kuhlee, A., Gatsogiannis, C., Balderhaar, H.J., Honscher, C., Engelbrecht-Vandre, S., *et al*. (2012). Molecular architecture of the multisubunit homotypic fusion and vacuole protein sorting (HOPS) tethering complex. *Proc Natl Acad Sci U S A* **109,** 1991-1996.

Brydges, S.D., Zhou, X.W., Huynh, M.H., Harper, J.M., Mital, J., Adjogble, K.D., *et al*. (2006). Targeted deletion of MIC5 enhances trimming proteolysis of *Toxoplasma* invasion proteins. *Eukaryot Cell* **5,** 2174-2183.

Budhidarmo, R., Nakatani, Y. and Day, C.L. (2012). RINGs hold the key to ubiquitin transfer. *Trends Biochem Sci* **37,** 58-65.

Cabrera, M., Arlt, H., Epp, N., Lachmann, J., Griffith, J., Perz, A., *et al*. (2013). Functional separation of endosomal fusion factors and the class C core vacuole/endosome tethering (CORVET) complex in endosome biogenesis. *J Biol Chem* **288,** 5166-5175.

Cerede, O., Dubremetz, J.F., Bout, D. and Lebrun, M. (2002). The *Toxoplasma gondii* protein MIC3 requires pro-peptide cleavage and dimerization to function as adhesin. *EMBO J* **21,** 2526-2536.

Couvreur, G., Sadak, A., Fortier, B. and Dubremetz, J.F. (1988). Surface antigens of *Toxoplasma gondii*. *Parasitology* **97,** 1-10.

Cullinane, A.R., Schaffer, A.A. and Huizing, M. (2013). The BEACH is hot: a LYST of emerging roles for BEACH-domain containing proteins in human disease. *Traffic* **14,** 749-766.

Daher, W., Plattner, F., Carlier, M.F. and Soldati-Favre, D. (2010). Concerted action of two formins in gliding motility and host cell invasion by *Toxoplasma gondii*. *PLoS Pathog* **6,** e1001132.

Di Cristina, M., Dou, Z., Lunghi, M., Kannan, G., Huynh, M.H., McGovern, O.L., *et al*. (2017). *Toxoplasma* depends on lysosomal consumption of autophagosomes for persistent infection. *Nat Microbiol* **2,** 17096.

Dogga, S.K., Mukherjee, B., Jacot, D., Kockmann, T., Molino, L., Hammoudi, P.M., *et al*. (2017). A druggable secretory protein maturase of *Toxoplasma* essential for invasion and egress. *Elife* **6,** e27480.

Donald, R.G. and Roos, D.S. (1993). Stable molecular transformation of *Toxoplasma gondii*: a selectable dihydrofolate reductase-thymidylate synthase marker based on drug-resistance mutations in malaria. *Proc Natl Acad Sci U S A* **90,** 11703-11707.

Dou, Z., Coppens, I. and Carruthers, V.B. (2013). Non-canonical maturation of two papain-family proteases in *Toxoplasma gondii*. *J Biol Chem* **288,** 3523-3534.

Dou, Z., McGovern, O.L., Di Cristina, M. and Carruthers, V.B. (2014). *Toxoplasma gondii* ingests and digests host cytosolic proteins. *MBio* **5,** e01188-01114.

Frenal, K., Dubremetz, J.F., Lebrun, M. and Soldati-Favre, D. (2017). Gliding motility powers invasion and egress in Apicomplexa. *Nat Rev Microbiol* **15,** 645-660.

Frenal, K., Polonais, V., Marq, J.B., Stratmann, R., Limenitakis, J. and Soldati-Favre, D. (2010). Functional dissection of the apicomplexan glideosome molecular architecture. *Cell Host Microbe* **8,** 343-357.

Hajagos, B.E., Turetzky, J.M., Peng, E.D., Cheng, S.J., Ryan, C.M., Souda, P., *et al*. (2012). Molecular dissection of novel trafficking and processing of the *Toxoplasma gondii* rhoptry metalloprotease toxolysin-1. *Traffic* **13,** 292-304.

Hakimi, M.A. and Bougdour, A. (2015). *Toxoplasma's* ways of manipulating the host transcriptome via secreted effectors. *Curr Opin Microbiol* **26,** 24-31.

Hakimi, M.A., Olias, P. and Sibley, L.D. (2017). *Toxoplasma* Effectors Targeting Host Signaling and Transcription. *Clin Microbiol Rev* **30,** 615-645.

Herm-Gotz, A., Agop-Nersesian, C., Munter, S., Grimley, J.S., Wandless, T.J., Frischknecht, F. and Meissner, M. (2007). Rapid control of protein level in the apicomplexan *Toxoplasma gondii*. *Nat Methods* **4,** 1003-1005.

Hoane, J.S., Carruthers, V.B., Striepen, B., Morrison, D.P., Entzeroth, R. and Howe, D.K. (2003). Analysis of the *Sarcocystis neurona* microneme protein SnMIC10: protein characteristics and expression during intracellular development. *Int J Parasitol* **33,** 671-679.

Horazdovsky, B.F., Cowles, C.R., Mustol, P., Holmes, M. and Emr, S.D. (1996). A novel RING finger protein, Vps8p, functionally interacts with the small GTPase, Vps21p, to facilitate soluble vacuolar protein localization. *J Biol Chem* **271,** 33607-33615.

Hunter, M.R., Scourfield, E.J., Emmott, E. and Graham, S.C. (2017). VPS18 recruits VPS41 to the human HOPS complex via a RING-RING interaction. *Biochem J* **474,** 3615-3626.

Huynh, M.H. and Carruthers, V.B. (2009). Tagging of endogenous genes in a *Toxoplasma gondii* strain lacking Ku80. *Eukaryot Cell* **8,** 530-539.

Huynh, M.H. and Carruthers, V.B. (2016). A *Toxoplasma gondii* Ortholog of *Plasmodium* GAMA Contributes to Parasite Attachment and Cell Invasion. *mSphere* **1,** e00012-16.

Jackson, A.J., Clucas, C., Mamczur, N.J., Ferguson, D.J. and Meissner, M. (2013). *Toxoplasma gondii* Syntaxin 6 is required for vesicular transport between endosomal-like compartments and the Golgi complex. *Traffic* **14,** 1166-1181.

Jimenez-Ruiz, E., Morlon-Guyot, J., Daher, W. and Meissner, M. (2016). Vacuolar protein sorting mechanisms in apicomplexan parasites. *Mol Biochem Parasitol* **209,** 18-25.

Kafsack, B.F., Pena, J.D., Coppens, I., Ravindran, S., Boothroyd, J.C. and Carruthers, V.B. (2009). Rapid membrane disruption by a perforin-like protein facilitates parasite exit from host cells. *Science* **323,** 530-533.

Kemp, L.E., Yamamoto, M. and Soldati-Favre, D. (2013). Subversion of host cellular functions by the apicomplexan parasites. *FEMS Microbiol Rev* **37,** 607-631.

Kim, K., Soldati, D. and Boothroyd, J.C. (1993). Gene replacement in *Toxoplasma gondii* with chloramphenicol acetyltransferase as selectable marker. *Science* **262,** 911-914.

Kremer, K., Kamin, D., Rittweger, E., Wilkes, J., Flammer, H., Mahler, S., *et al*. (2013). An overexpression screen of *Toxoplasma gondii* Rab-GTPases reveals distinct transport routes to the micronemes. *PLoS Pathog* **9,** e1003213.

Lamarque, M.H., Roques, M., Kong-Hap, M., Tonkin, M.L., Rugarabamu, G., Marq, J.B., *et al*. (2014). Plasticity and redundancy among AMA-RON pairs ensure host cell entry of *Toxoplasma* parasites. *Nat Commun* **5,** 4098.

Larson, E.T., Parussini, F., Huynh, M.H., Giebel, J.D., Kelley, A.M., Zhang, L., *et al*. (2009). *Toxoplasma gondii* cathepsin L is the primary target of the invasion-inhibitory compound morpholinurea-leucyl-homophenyl-vinyl sulfone phenyl. *J Biol Chem* **284,** 26839-26850.

Lebrun, M., Michelin, A., El Hajj, H., Poncet, J., Bradley, P.J., Vial, H. and Dubremetz, J.F. (2005). The rhoptry neck protein RON4 re-localizes at the moving junction during *Toxoplasma gondii* invasion. *Cell Microbiol* **7,** 1823-1833.

Lentini, G., El Hajj, H., Papoin, J., Fall, G., Pfaff, A.W., Tawil, N., *et al*. (2017). Characterization of *Toxoplasma* DegP, a rhoptry serine protease crucial for lethal infection in mice. *PLoS One* **12,** e0189556.

Leriche, M.A. and Dubremetz, J.F. (1991). Characterization of the protein contents of rhoptries and dense granules of *Toxoplasma gondii* tachyzoites by subcellular fractionation and monoclonal antibodies. *Mol Biochem Parasitol* **45,** 249-259.

Liu, Q., Li, F.C., Zhou, C.X. and Zhu, X.Q. (2017). Research advances in interactions related to *Toxoplasma gondii* microneme proteins. *Exp Parasitol* **176,** 89-98.

Lorincz, P., Lakatos, Z., Varga, A., Maruzs, T., Simon-Vecsei, Z., Darula, Z., *et al*. (2016). MiniCORVET is a Vps8-containing early endosomal tether in *Drosophila*. *Elife* **5,** e14226.

Markgraf, D.F., Ahnert, F., Arlt, H., Mari, M., Peplowska, K., Epp, N., *et al*. (2009). The CORVET subunit Vps8 cooperates with the Rab5 homolog Vps21 to induce clustering of late endosomal compartments. *Mol Biol Cell* **20,** 5276-5289.

McGovern, O.L., Rivera-Cuevas, Y., Kannan, G., Narwold, A., Jr. and Carruthers, V.B. (2018). Intersection of Endocytic and Exocytic Systems in *Toxoplasma gondii*. *Traffic* **19,** 336-353.

Meissner, M., Brecht, S., Bujard, H. and Soldati, D. (2001). Modulation of myosin A expression by a newly established tetracycline repressor-based inducible system in *Toxoplasma gondii*. *Nucleic Acids Res* **29,** E115.

Mercier, C. and Cesbron-Delauw, M.F. (2015). *Toxoplasma* secretory granules: one population or more? *Trends Parasitol* **31,** 604.

Miller, S.A., Binder, E.M., Blackman, M.J., Carruthers, V.B. and Kim, K. (2001). A conserved subtilisin-like protein TgSUB1 in microneme organelles of *Toxoplasma gondii*. *J Biol Chem* **276,** 45341-45348.

Miller, S.A., Thathy, V., Ajioka, J.W., Blackman, M.J. and Kim, K. (2003). TgSUB2 is a *Toxoplasma gondii* rhoptry organelle processing proteinase. *Mol Microbiol* **49,** 883-894.

Mima, J., Hickey, C.M., Xu, H., Jun, Y. and Wickner, W. (2008). Reconstituted membrane fusion requires regulatory lipids, SNAREs and synergistic SNARE chaperones. *EMBO J* **27,** 2031-2042.

Morlon-Guyot, J., Berry, L., Chen, C.T., Gubbels, M.J., Lebrun, M. and Daher, W. (2014). The *Toxoplasma gondii* calcium-dependent protein kinase 7 is involved in early steps of parasite division and is crucial for parasite survival. *Cell Microbiol* **16,** 95-114.

Morlon-Guyot, J., Pastore, S., Berry, L., Lebrun, M. and Daher, W. (2015). *Toxoplasma gondii* Vps11, a subunit of HOPS and CORVET tethering complexes, is essential for the biogenesis of secretory organelles. *Cell Microbiol* **17,** 1157-1178.

Mueller, C., Klages, N., Jacot, D., Santos, J.M., Cabrera, A., Gilberger, T.W., *et al*. (2013). The *Toxoplasma* protein ARO mediates the apical positioning of rhoptry organelles, a prerequisite for host cell invasion. *Cell Host Microbe* **13,** 289-301.

Mueller, C., Samoo, A., Hammoudi, P.M., Klages, N., Kallio, J.P., Kursula, I. and Soldati-Favre, D. (2016). Structural and functional dissection of *Toxoplasma gondii* armadillo repeats only protein. *J Cell Sci* **129,** 1031-1045.

Nagle, D.L., Karim, M.A., Woolf, E.A., Holmgren, L., Bork, P., Misumi, D.J., *et al*. (1996). Identification and mutation analysis of the complete gene for Chediak-Higashi syndrome. *Nat Genet* **14,** 307-311.

Nickerson, D.P., Brett, C.L. and Merz, A.J. (2009). Vps-C complexes: gatekeepers of endolysosomal traffic. *Curr Opin Cell Biol* **21,** 543-551.

Nishi, M., Hu, K., Murray, J.M. and Roos, D.S. (2008). Organellar dynamics during the cell cycle of *Toxoplasma gondii*. *J Cell Sci* **121,** 1559-1568.

Ostrowicz, C.W., Brocker, C., Ahnert, F., Nordmann, M., Lachmann, J., Peplowska, K., *et al*. (2010). Defined subunit arrangement and rab interactions are required for functionality of the HOPS tethering complex. *Traffic* **11,** 1334-1346.

Ostrowicz, C.W., Meiringer, C.T. and Ungermann, C. (2008). Yeast vacuole fusion: a model system for eukaryotic endomembrane dynamics. *Autophagy* **4,** 5-19.

Parker, M.L., Penarete-Vargas, D.M., Hamilton, P.T., Guerin, A., Dubey, J.P., Perlman, S.J., *et al*. (2016). Dissecting the interface between apicomplexan parasite and host cell: Insights from a divergent AMA-RON2 pair. *Proc Natl Acad Sci U S A* **113,** 398-403.

Parussini, F., Coppens, I., Shah, P.P., Diamond, S.L. and Carruthers, V.B. (2010). Cathepsin L occupies a vacuolar compartment and is a protein maturase within the endo/exocytic system of *Toxoplasma gondii*. *Mol Microbiol* **76,** 1340-1357.

Pelletier, L., Stern, C.A., Pypaert, M., Sheff, D., Ngo, H.M., Roper, N., *et al*. (2002). Golgi biogenesis in *Toxoplasma gondii*. *Nature* **418,** 548-552.

Peplowska, K., Markgraf, D.F., Ostrowicz, C.W., Bange, G. and Ungermann, C. (2007). The CORVET tethering complex interacts with the yeast Rab5 homolog Vps21 and is involved in endo-lysosomal biogenesis. *Dev Cell* **12,** 739-750.

Pieperhoff, M.S., Schmitt, M., Ferguson, D.J. and Meissner, M. (2013). The role of clathrin in post-Golgi trafficking in *Toxoplasma gondii*. *PLoS One* **8,** e77620.

Plemel, R.L., Lobingier, B.T., Brett, C.L., Angers, C.G., Nickerson, D.P., Paulsel, A., *et al*. (2011). Subunit organization and Rab interactions of Vps-C protein complexes that control endolysosomal membrane traffic. *Mol Biol Cell* **22,** 1353-1363.

Raposo, G., Marks, M.S. and Cutler, D.F. (2007). Lysosome-related organelles: driving post-Golgi compartments into specialisation. *Curr Opin Cell Biol* **19,** 394-401.

Raymond, C.K., Howald-Stevenson, I., Vater, C.A. and Stevens, T.H. (1992). Morphological classification of the yeast vacuolar protein sorting mutants: evidence for a prevacuolar compartment in class E vps mutants. *Mol Biol Cell* **3,** 1389-1402.

Reiss, M., Viebig, N., Brecht, S., Fourmaux, M.N., Soete, M., Di Cristina, M., *et al*. (2001). Identification and characterization of an escorter for two secretory adhesins in *Toxoplasma gondii*. *J Cell Biol* **152,** 563-578.

Ren, Y., Yip, C.K., Tripathi, A., Huie, D., Jeffrey, P.D., Walz, T. and Hughson, F.M. (2009). A structure-based mechanism for vesicle capture by the multisubunit tethering complex Dsl1. *Cell* **139,** 1119-1129.

Sakura, T., Sindikubwabo, F., Oesterlin, L.K., Bousquet, H., Slomianny, C., Hakimi, M.A., *et al*. (2016). A Critical Role for *Toxoplasma gondii* Vacuolar Protein Sorting VPS9 in Secretory Organelle Biogenesis and Host Infection. *Sci Rep* **6,** 38842.

Sangare, L.O., Alayi, T.D., Westermann, B., Hovasse, A., Sindikubwabo, F., Callebaut, I., *et al*. (2016). Unconventional endosome-like compartment and retromer complex in *Toxoplasma gondii* govern parasite integrity and host infection. *Nat Commun* **7,** 11191.

Seals, D.F., Eitzen, G., Margolis, N., Wickner, W.T. and Price, A. (2000). A Ypt/Rab effector complex containing the Sec1 homolog Vps33p is required for homotypic vacuole fusion. *Proc Natl Acad Sci U S A* **97,** 9402-9407.

Shaw, M.K., Roos, D.S. and Tilney, L.G. (1998). Acidic compartments and rhoptry formation in *Toxoplasma gondii*. *Parasitology* **117,** 435-443.

Sheiner, L., Demerly, J.L., Poulsen, N., Beatty, W.L., Lucas, O., Behnke, M.S., *et al*. (2011). A systematic screen to discover and analyze apicoplast proteins identifies a conserved and essential protein import factor. *PLoS Pathog* **7,** e1002392.

Sidik, S.M., Huet, D., Ganesan, S.M., Huynh, M.H., Wang, T., Nasamu, A.S., *et al*. (2016). A Genome-wide CRISPR Screen in *Toxoplasma* Identifies Essential Apicomplexan Genes. *Cell* **166,** 1423-1435.e1412.

Sloves, P.J., Delhaye, S., Mouveaux, T., Werkmeister, E., Slomianny, C., Hovasse, A., *et al*. (2012). *Toxoplasma* sortilin-like receptor regulates protein transport and is essential for apical secretory organelle biogenesis and host infection. *Cell Host Microbe* **11,** 515-527.

Soldati, D., Lassen, A., Dubremetz, J.F. and Boothroyd, J.C. (1998). Processing of *Toxoplasma* ROP1 protein in nascent rhoptries. *Mol Biochem Parasitol* **96,** 37-48.

Solinger, J.A. and Spang, A. (2013). Tethering complexes in the endocytic pathway: CORVET and HOPS. *FEBS J* **280,** 2743-2757.

Spang, A. (2016). Membrane Tethering Complexes in the Endosomal System. *Front Cell Dev Biol* **4,** 35.

Sparvoli, D., Richardson, E., Osakada, H., Lan, X., Iwamoto, M., Bowman, G.R., *et al*. (2018). Remodeling the Specificity of an Endosomal CORVET Tether Underlies Formation of Regulated Secretory Vesicles in the Ciliate *Tetrahymena thermophila*. *Curr Biol* **28,** 697-710.e13.

Sudhof, T.C. and Rothman, J.E. (2009). Membrane fusion: grappling with SNARE and SM proteins. *Science* **323,** 474-477.

Torres, V.A., Mielgo, A., Barila, D., Anderson, D.H. and Stupack, D. (2008). Caspase 8 promotes peripheral localization and activation of Rab5. *J Biol Chem* **283,** 36280-36289.

Turetzky, J.M., Chu, D.K., Hajagos, B.E. and Bradley, P.J. (2010). Processing and secretion of ROP13: A unique *Toxoplasma* effector protein. *Int J Parasitol* **40,** 1037-1044.

van der Kant, R., Jonker, C.T., Wijdeven, R.H., Bakker, J., Janssen, L., Klumperman, J. and Neefjes, J. (2015). Characterization of the Mammalian CORVET and HOPS Complexes and Their Modular Restructuring for Endosome Specificity. *J Biol Chem* **290,** 30280-30290.

Venugopal, K., Werkmeister, E., Barois, N., Saliou, J.M., Poncet, A., Huot, L., *et al*. (2017). Dual role of the *Toxoplasma gondii* clathrin adaptor AP1 in the sorting of rhoptry and microneme proteins and in parasite division. *PLoS Pathog* **13,** e1006331.

Wisniewski, J.R., Zougman, A., Nagaraj, N. and Mann, M. (2009). Universal sample preparation method for proteome analysis. *Nat Methods* **6,** 359-362.

Zlatic, S.A., Tornieri, K., L'Hernault, S.W. and Faundez, V. (2011). Clathrin-dependent mechanisms modulate the subcellular distribution of class C Vps/HOPS tether subunits in polarized and nonpolarized cells. *Mol Biol Cell* **22,** 1699-1715.

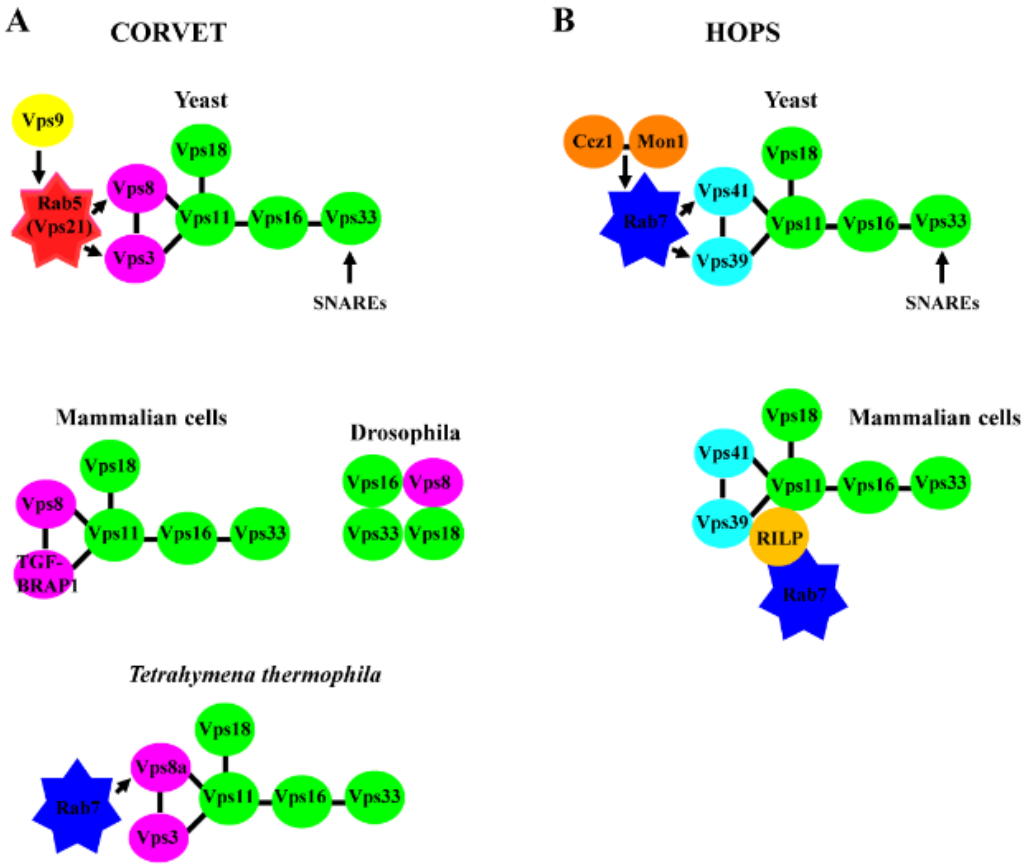

Figure 1. (A - B). Models depicting the compositions of CORVET and HOPS complexes in Yeast, Mammalian cells, *Drosophila* and *Tetrahymena*. Common subunits are colored green, violets and blues are specific to CORVET and HOPS respectively. Classically, the CORVET complex binds to Rab5 on early endosomes whereas the HOPS complex via Rab7 is associated with late endosomes. In mammalian cells, the CORVET complex is maintained by TGFBRAP1 which interacts with Vps11 and prevents its association with RILP known to bind Rab7. The conversion of CORVET to HOPS complex from Rab5- to Rab7- during endosomal maturation occurs when both TGFBRAP1 and Vps8 are replaced by Vps39 and Vps41 respectively. RILP interacts with Vps41, Vps39, Vps11 and Rab7 proteins. In *Drosophila*, the unconventional CORVET complex is composed of only four sub-units. *Tetrahymena* expresses only a CORVET complex and surprisingly Vps8a binds to Rab7. RILP: Rab-interacting lysosomal protein. TGFBRAP1: Transforming Growth Factor Beta Receptor Associated Protein 1.

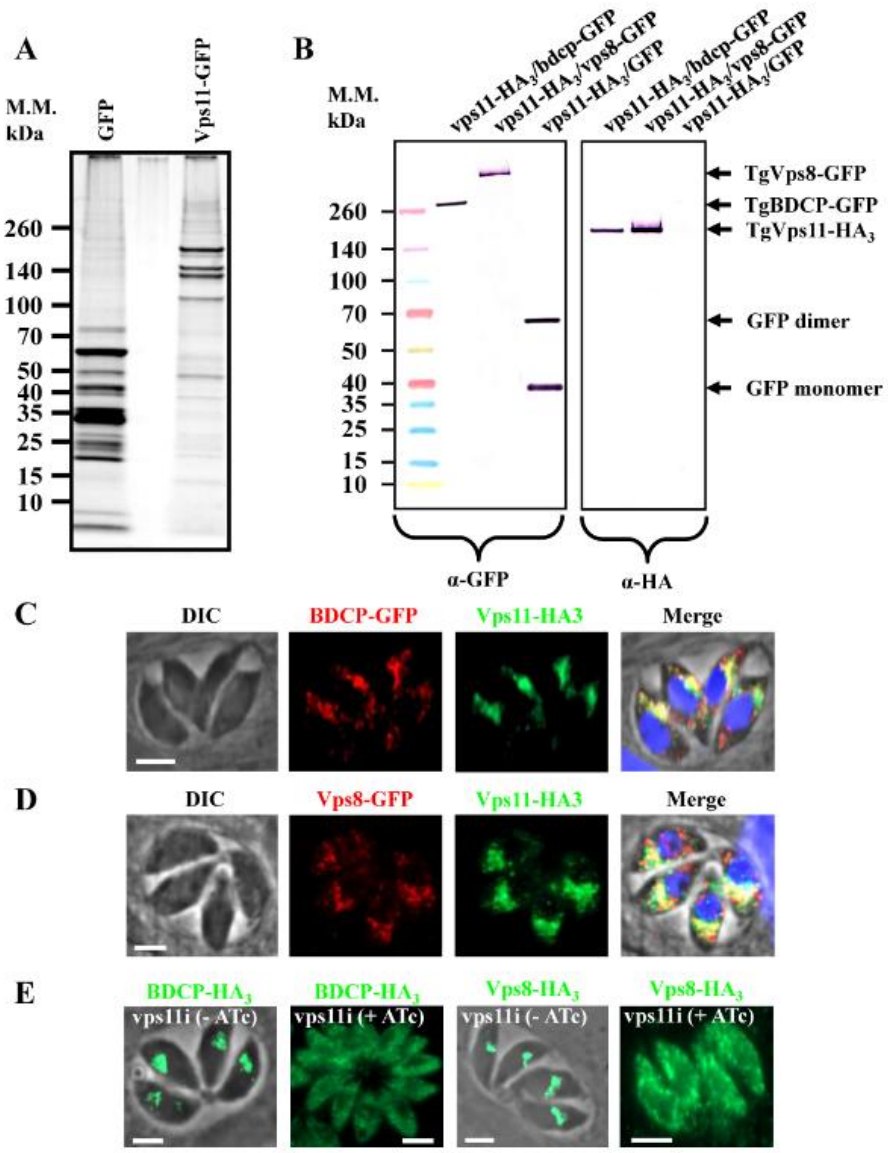

Figure 2. TgBDCP and TgVps8 belong to the interaction network of CORVET and HOPS tethering complexes. (A). Silver-stained gel showing several bands that were detected after immuno-precipitation using anti-GFP antibodies. Parasite strain stably expressing GFP was used as negative control. Both eluates from GFP and Vps11-GFP beads were subjected to mass spectrometry (MS) analysis. MS results are listed in both table 1 and supplementary table 1. **(B).** The endogenous proteins TgBDCP or TgVps8 and TgVps11 were fused to a GFP and 3-HA tags, respectively (2 first lines). GFP protein alone and the native TgVps11 protein fused to 3-HA tags was used as negative control (3rd line). Pull-down experiments were carried out using the GFP-Trap system. Proteins that bind to GFP or to TgVps11-GFP were eluted and subjected to western blot analysis with anti-GFP (left lanes) and anti-HA (right lanes) antibodies. **(C and D).** Co-staining between GFP- tagged TgBDCP

and TgVps8 and endomembrane marker TgVps11. TgBDCP-GFP or TgVps8-GFP and TgVps11-HA_3 were detected using anti-GFP and anti-HA antibodies respectively. DIC: differential interference contrast. **(E).** Immuno-fluorescence assays of TgBDCP-HA_3 or TgVps8-HA_3 in intracellular vps11i parasites grown without or in the presence of ATc for 2 days. TgBDCP-HA_3 and TgVps8-HA_3 were detected using anti-HA antibodies.

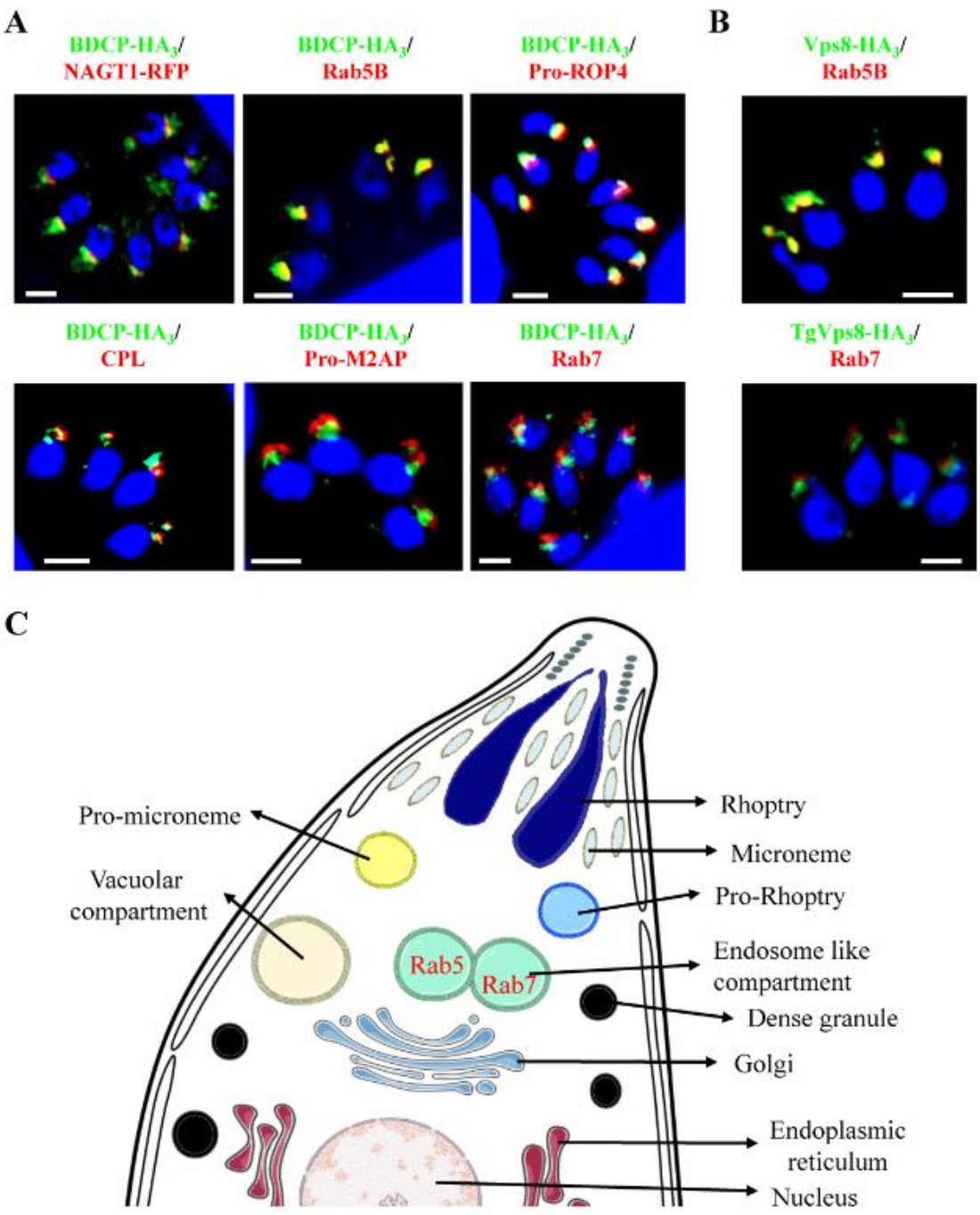

Figure 3. Expression and localization of TgBDCP and TgVps8 in tachyzoites. (A and B). Immunofluorescence analysis of TgBDCP-HA_3 and TgVps8-HA_3 parasites grown on HFF monolayers, with the indicated antibodies (pro-ROP4, CPL and pro-M2AP) or transiently expressing the indicated markers (NAGT1-RFP, DD-Myc-Rab5B and DD-Myc-Rab7). The nucleus is shown in blue. Scale bars represent 2µm. **(C).** A parasite illustration showing the endocytic and exocytic systems of the parasite. The plasma membrane and the inner membrane complex are shown in black, the nucleus is pink, the early exocytic pathway (ER and Golgi) is shown in maroon and blue, the endocytic system (Rab5 (EE), Rab7 (LE), and

VAC) in green and light yellow, and the late exocytic system (pro-rhoptry, pro-microneme, micronemes and rhoptries) in different types of blue and yellow.

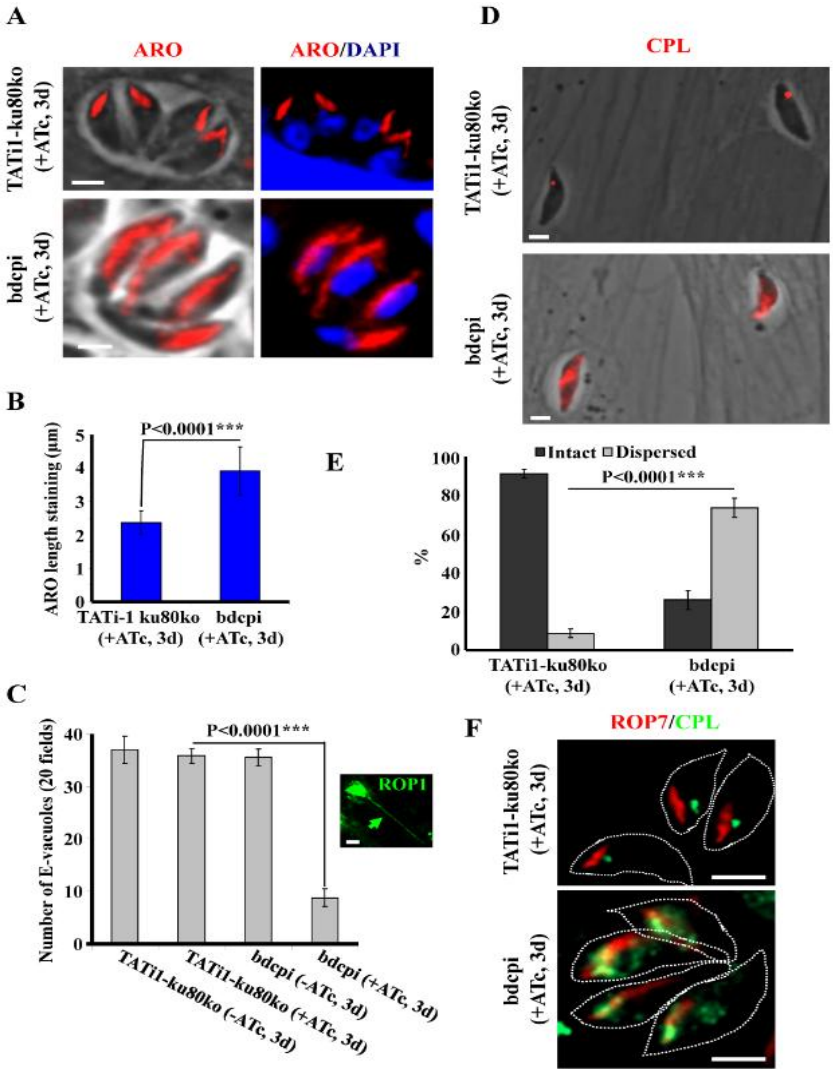

Figure 4. Depletion of TgBDCP impairs Lysosome-Related Organelles (rhoptries and VAC) of the parasite. (A). Immunofluorescence analyses of wild-type (TATi1-ku80ko) and bdcpi strains grown for 72 hrs with ATc. Immunofluorescence was performed with anti-ARO polyclonal antibodies and revealed an unusual elongated membranous structures staining. The nucleus is shown in blue (DAPI). IFA scale bars represent 2 μm. **(B).** Histogram plots of ARO staining length in wild-type (TATi1-ku80ko) and bdcpi strains grown for 72 hrs with ATc. Data are presented as mean ± S.D. of three independent experiments. **(C).** Scoring the number of E-vacuoles in the parental (TATi1-ku80ko) and inducible knockdown TgBDCP cell lines treated with ± ATc. The number of E-vacuoles in 20 fields were counted following IFA using anti-ROP1 antibodies. Data are mean values ± S.D. for three independent experiments. IFA scale bars represent 2 μm. **(D).** Loss of TgBDCP results in dispersion of the CPL staining probably due to the enlargement of the VAC. Representative images of wild-type (TATi1-ku80ko) and bdcpi parasites grown in the presence of ATc for 72 hrs and labeled with anti-CPL antibodies to highlight the VAC. IFA scale bars represent 2 μm. **(E).**

Quantification of intact or dispersed CPL staining in the parental (TATi1-ku80ko) and inducible knockdown TgBDCP cell lines treated with ATc for 72 hrs. Data are mean values ± S.D. for three independent experiments. **(F).** Immunofluorescence analyses of wild-type (TATi1-ku80ko) and bdcpi strains grown for 72 hrs with ATc. Immunofluorescence was performed with both anti-ROP7 and anti-CPL antibodies and revealed an unusual colocalization between both organelles markers in absence of BDCP protein. IFA scale bars represent 2 μm.

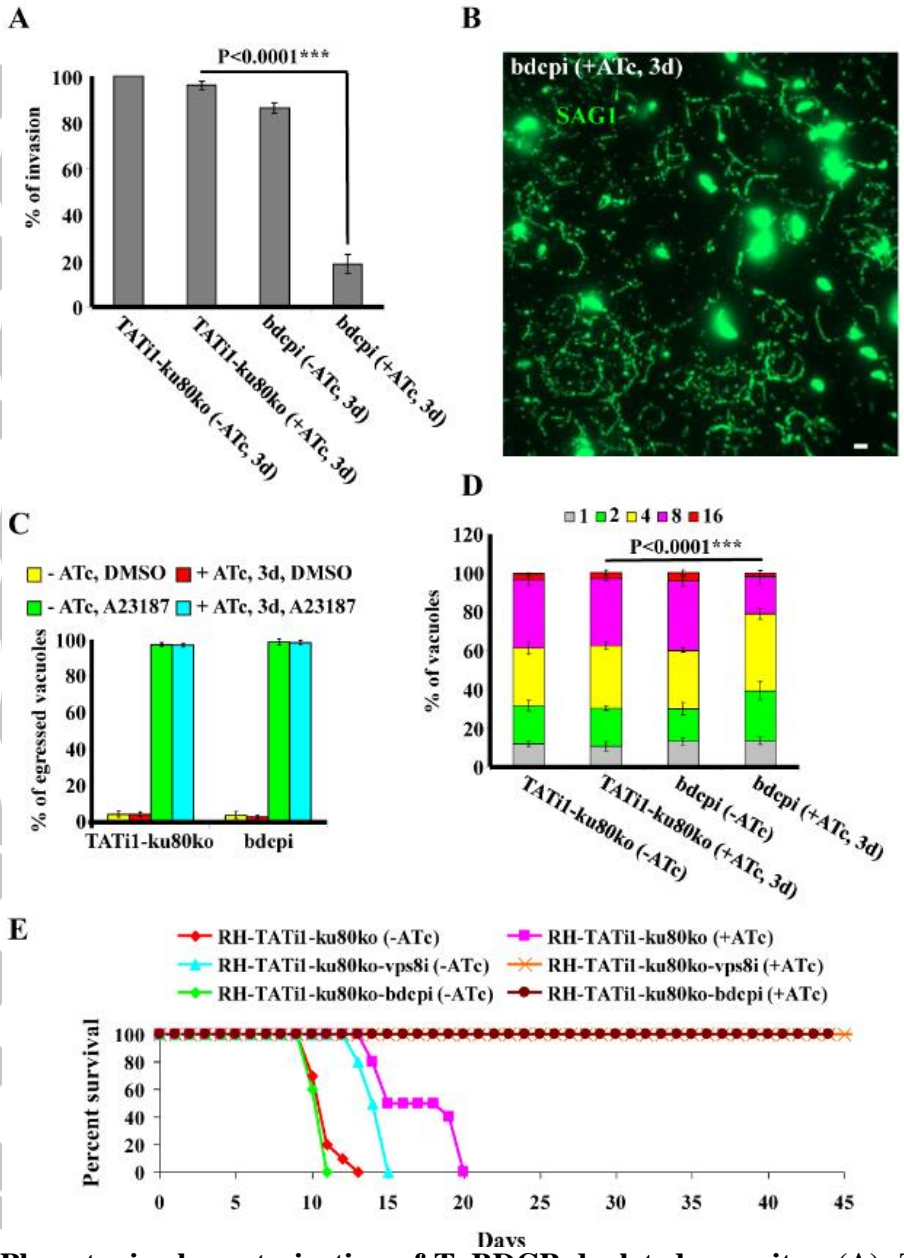

Figure 5. Phenotypic characterization of TgBDCP-depleted parasites. (A). The invasion capacity of Tgbdcpi and parental (TATi1-ku80ko) parasites was evaluated after 3 days ± ATc. Results are expressed as percentage of invading parasites and represented as mean ± S.D. **(B).** Gliding motility was assessed after growing Tgbdcpi mutant parasites for a total of 3 days + ATc. Parasites were added to Poly-L-Lysine pretreated coverslips, and trails were visualized using anti-SAG1 antibodies. IFA scale bars represent 2 μm. **(C).** Egress assay was performed by growing parasites for 3 days ±ATc. Egress was induced upon addition of 3 μM A23187, and DMSO was used as a negative control. The data shown are mean values ± S.D. from three independent experiments. **(D).** Intracellular growth of TATi1-ku80ko and Tgbdcpi cultivated in presence or absence of ATc for 2 days and allowed to invade new HFF cells.

Numbers of parasites per vacuole (x-axis) were counted 24 hrs after inoculation. The percentages of vacuoles containing varying numbers of parasites are represented on the y-axis. Values are means ± S.D. for three independent experiments. **(E).** Knock-down of TgBDCP or TgVps8 protein suppresses parasite virulence in a mouse model. One hundred tachyzoites of the indicated strains were injected into Balb-c mice (n = 10), and mouse survival was monitored daily (ATc was added or not in the mice drinking water).

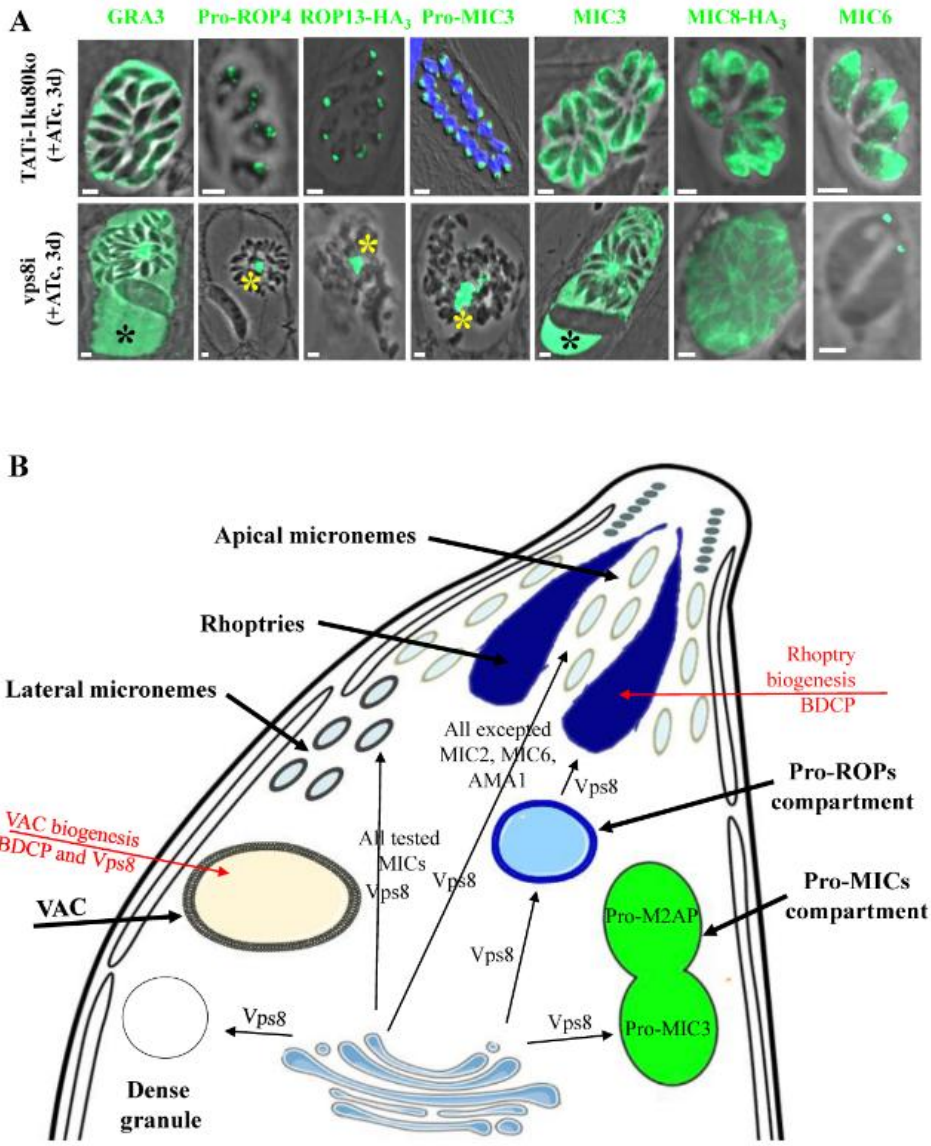

Figure 6. TgVps8 is required for the transport of dense granules, micronemal and rhoptry proteins. (A). Immunofluorescence analysis of TATi1-ku80ko or vps8i parasites grown in the presence of ATc for 3 days. GRA3, pro-ROP4, pro-MIC3, MIC3 and MIC6 proteins were stained with the indicated antibodies. ROP13-HA_3 and MIC8-HA_3 proteins were visualized using anti-HA antibodies. The dense granule 3 (GRA3) protein, the premature rhoptry protein (pro-ROP4), the rhoptry bulb protein (ROP13), the premature micronemal protein (pro-MIC3) and several microneme proteins including MIC3, MIC8 and MIC6 were mistargeted to different locations in TgVps8-depleted parasites. Mislocalizations (host cell cytoplasm or residual body) are indicated by different coloured asterisks. In TgVps8-depleted parasites, MIC8 associates to the pellicle and MIC6 accumulates at the apex. As expected, all studied proteins were correctly localized in TATi1-ku80ko wild-type parasites treated with ATc. Scale bars represent 2µm. **(B).** A model that summarizes the

functions of TgBDCP in the biogenesis of parasite LROs and TgVps8 in the transport of proteins to different secretory organelles. Our results indicate a role of TgBDCP in maintaining the integrity of rhoptries and VAC. TgVps8 plays a more vital role in transporting proteins to dense granules, rhoptries, lateral micronems and towards a sub-compartment of pro-micronemes. In contrast, routing of pro-M2AP to pre-micronemes and MIC2, MIC6 and AMA1 to apical micronemes are not affected. Finally TgVps8 seems to be involved in the biogenesis of VAC.

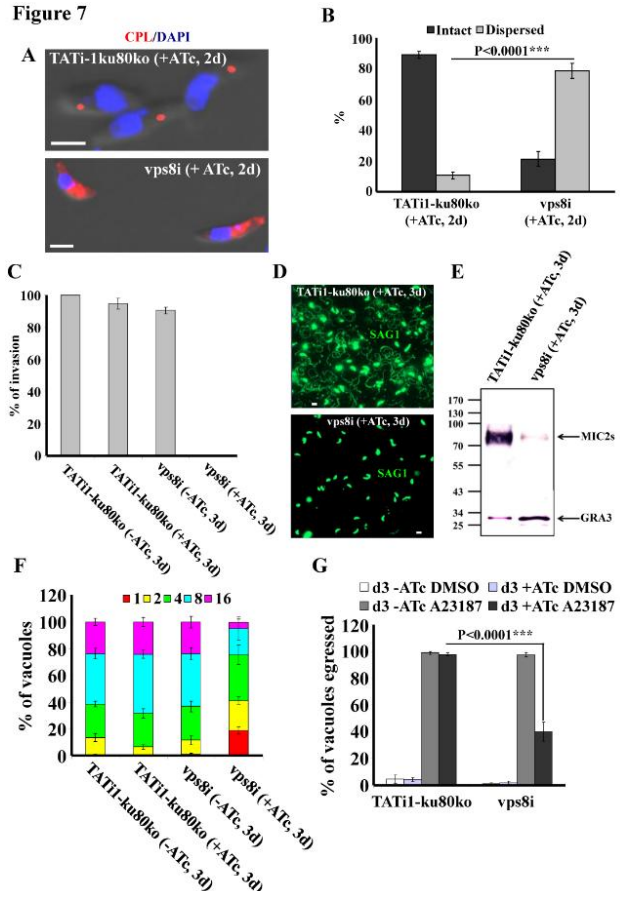

Figure 7. Disruption of TgVsp8 impairs the Lysosome-Related Organelle (VAC) of the parasite and phenotypic consequences of TgVps8 depletion in vps8i strain. (A). Loss of TgVps8 results in dispersion of the CPL staining probably due to the enlargement of the VAC. Representative images of wild-type (TATi1-ku80ko) and vps8i parasites grown in the presence of ATc for 48 hrs and labeled with anti-CPL antibodies to highlight the VAC. The nucleus is shown in blue (DAPI). IFA scale bars represent 2 μm. **(B).** Quantification of intact or dispersed CPL staining in the parental (TATi1-ku80ko) and inducible knock-down TgVps8 cell lines treated with ATc for 48 hrs. Data are mean values ± S.D. for three independent experiments. **(C, D, E, F and G).** All assays described here were performed with TATi1-ku80ko and vps8i grown for a total of 72 hrs ± ATc. **(C).** Invasion assay performed on TATi1-ku80ko or vps8i strains ± ATc. The percentage of parasites that have invaded host cells at day 3 is represented. Values represent means ± S.D. from three independent experiments. **(D).** Gliding motility was assessed after growing parasites for a total of 72 hrs + ATc. Parasites were added to Poly-L-Lysine pretreated coverslips, and trails were visualized using anti-SAG1 antibodies. Scale bars represent 2µm. **(E).** Microneme secretion assay was performed on wild-type (TATi1-ku80ko) and Tgvps8i lines treated with ATc for 3 days. TgVps8-depleted parasites are not able to secrete their micronemes as indicated by the

absence of signal when ESA (excreted secretory antigens/micronemes) was probed for MIC2 micronemal protein. Secreted MIC2s is detected at around ~85 kDa. Microneme secretion was triggered in presence of propranolol (500 mM). Dense granule protein 3 (GRA3) was used as control for constitutive secretion. MIC2s: secreted. **(F).** Intracellular growth assay was carried out after 72 hrs of parasite growth ± ATc. IFA was performed with anti-GAP45 antibodies and the number of parasites per vacuole was counted. Values represent means ± S.D. from three independent experiments. **(G).** Egress assay was performed by growing parasites for 72 hrs ± ATc. Egress was induced upon addition of 3 μM A23187, and DMSO was used as a negative control. The data shown are mean values ± S.D. from three independent experiments.

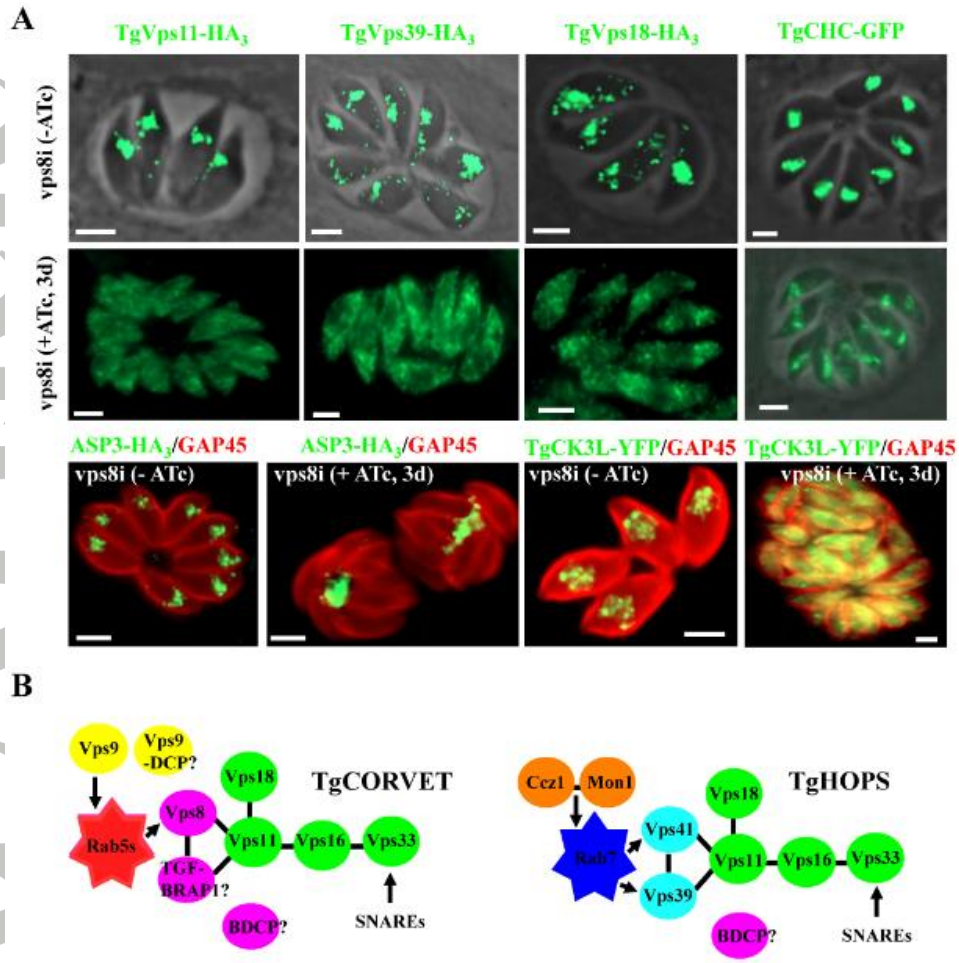

Figure 8. (A). TgVps8 dictates the correct targeting of *Toxoplasma* Vps11, Vps39, Vps18, CHC, ASP3 and CK3L proteins. Immunofluorescence assays of Vps11-HA_3, Vps39-HA_3, Vps18-HA_3, CHC-GFP, ASP3-HA_3 and CK3L-GFP in intracellular vps8i parasites grown without or in the presence of ATc for 3 days. Vps11 and Vps39 and Vps18 or CHC or ASP3 or CK3L were detected using either anti-HA or anti-GFP antibodies, respectively. Anti-GAP45 antibodies were used to stain the pellicle of parasites. Scale bars represent 2µm. **(B).** A putative model showing the different subunits that constitute the CORVET and HOPS complexes in *Toxoplasma*. Mass spectrometry analysis allowed us to identify the Vps8 subunit that we were missing (Morlon-Guyot *et al*., 2015). The presence or absence of Vps3 remains a mystery, but a comparative analysis based on sequence homology allowed us to identify a homologue of TGFBRAP1 in *Toxoplasma*. This latter protein associates with CORVET in mammalian cells and replaces Vps39 (van der Kant *et al*., 2015). Interestingly, this study has unveiled two new proteins that may be part of the CORVET complex called Vps9-DCP and BDCP. Our results demonstrated a convincing colocalization between BDCP and Rab5B suggesting that BDCP is likely to belong to CORVET. However,

we cannot rule out that the BDCP protein transiently associates with the HOPS complex to perform its function related to the biogenesis of the VAC compartment and mature rhoptries. Concerning proteins that contain a Vps9 domain, they are known to mediate the association and dissociation of Rab5 from membranes. Thus these analyzes may suggest an atypical organization of the CORVET complex in *Toxoplasma*. Finally the HOPS complex of the parasite *Toxoplasma* seems to resemble the structure of the same complex described in yeast (Balderhaar *et al*., 2013, Brocker *et al*., 2012).

Table 1: Composition of CORVET and HOPS complexes in *Toxoplasma gondii*.

			Total number of unique peptides		
Protein name	**Accession numbers and phenotypic score**	**Molecular weight (kDa)**	**IP1**	**IP2**	**Control**
Vps39 (HOPS specific)	TGME49_315530 (-4.2)	126	27	28	0
Vps11	TGME49_230220 (-4.1)	137	23	16	0
Vps18	TGME49_289730 (-3.2)	128	17	13	0
Vps16	TGME49_320670 (-4.8)	102	14	10	0
Vps33	TGME49_295000 (-4.8)	111	12	9	0
Vps8 (CORVET specific)	TGME49_289520 (-4.9)	356	10	11	0
Vps41 (HOPS specific)	TGME49_224270 (-3.8)	358	8	10	0
Vps9-DCP	TGME49_281570 (-0.2)	53	6	8	0
BDCP	TGME49_263000 (-0.9)	207	5	1	0
Hypothetical protein	TGME49_313340 (-0.2)	161	1	1	0